EVALUATING THE ZOONOTIC POTENTIAL OF NON-HUMAN INFLUENZA D VIRUS

by

Kirsten Elizabeth Littlefield

A thesis submitted to Johns Hopkins University in conformity with the requirements for the degree of Master of Science

Baltimore, Maryland

April 2021

Abstract

Influenza viruses are respiratory pathogens known to infect a wide variety of vertebrate species and cause annual epidemics in addition to sporadic pandemics. These viruses belong to the *Orthomyxoviridae* family and are divided into three genera – influenzas A, B, and C. In 2011, a novel virus sharing approximately 50% amino acid homology with human influenza C virus (ICV) was isolated from pigs showing symptoms of respiratory infection in Oklahoma. Further studies revealed that this newly isolated virus was unable to reassort with human ICV to produce viable progeny and exhibited no cross-recognition with human ICV polyclonal antibodies. These findings suggested the virus isolate was genetically and antigenically divergent from human ICV, thus a new genus within the *Orthomyxoviridae* family was established, termed influenza D virus (IDV). In 2017 and 2018, the Animal Influenza Ecology and Epidemiology Research Program at The Ohio State University collected nasal swabs and nasal wipes from swine being sold at jackpot shows and identified several IDV strains. To investigate the potential for IDV transmission to humans, we infected primary human nasal epithelial cells (hNECs) with three swine isolates of IDV (D/swine/Kentucky/17TOSU1262/2017, D/swine/Ohio/18TOSU0287/2018, and D/swine/Kentucky/17SW1262/2017) and determined infectious virus production and epithelial cell tropism at temperatures consistent with the upper (32˚C) and lower (37˚C) human respiratory tract. The IDV strains replicated to high infectious virus titer in MDCK cells and hNEC cultures, indicating they were capable of infecting cells of the human respiratory tract. A comparison of chemokine and cytokine induction in hNEC cultures following IDV infection demonstrated decreased expression in 50% of factors tested when compared to ICV infected cultures. High titer replication in conjunction with repression of the innate immune response suggests IDV is capable of human infection. These studies provide a

better understanding of the ability of IDV to infect and cause disease in humans and suggest increased surveillance for this genus of influenza virus is necessary.

Primary Reader and Advisor: Andrew Pekosz, PhD

Secondary Reader: Sabra Klein, PhD

Acknowledgements

"If I have seen further, it is by standing on the shoulders of giants" ~Sir Isaac Newton
Having the privilege to study at the Bloomberg School of Public Health has shown me the truth of Sir Isaac Newton's words. During my time as a student at Johns Hopkins, my professors, lab mates, and friends have supported me and allowed me to achieve heights I could only dream of on my own. I would particularly like to thank my mentor, Dr. Andrew Pekosz. His guidance, confidence, and patience have been essential to my development as a scientist and to my success in the field of virology. I would also like to acknowledge my fellow researchers in the Pekosz Lab, who fostered a work environment that made me excited to come to lab every day and taught me everything I know about bench work. And to the friends I have made through this program, thank you for making Baltimore feel like home. Finally, I would like to thank my parents, without their unwavering support, consistent availability for 2 am phone calls, and caffeine filled care packages, my success in this program would have been impossible. These are the giants I have relied on and as I progress in the world of science, I hope to become a giant that can one day raise another high enough to see beyond what I have learned.

Table of Contents

LIST OF FIGURES

Chapter 1: Influenza D Virus Replication in Primary Human Nasal Epithelial Cell Cultures

INTRODUCTION

Introduction to Influenza D Virus

Influenza viruses are negative-sense, single-stranded, segmented RNA viruses belonging to the *Orthomyxoviridae* family. Prior to 2011, only three genera of influenza virus were known to exist, influenza A (IAV), B (IBV), and C (ICV) viruses[1]. IAV and IBV both possess 8 genomic segments that encode 11 proteins, including hemagglutinin (HA), neuraminidase (NA), matrix 1 (M1), matrix 2, nucleoprotein (NP), non-structural protein 1, non-structural protein 2, polymerase acid protein, polymerase basic protein 1 (PB1), polymerase basic protein 2, and polymerase basic protein 1-F2[2]. For IAV and IBV, HA serves to mediate receptor recognition and membrane fusion, whereas NA possesses receptor destroying functions[3,4]. This is in contrast to ICV whose genome consists of 7 genomic segments and encodes only one surface protein, hemagglutinin-esterase-fusion glycoprotein (HEF). The HEF protein combines the functions of the analogous HA and NA proteins, allowing for receptor binding, receptor destroying, and membrane fusion[4].

Influenza viruses are classified into the three genera according to two criteria[5]. First is the sequence homology of highly conserved proteins. Typically in phylogenetic analyses, the nucleotide sequence of either PB1 or NP and M1 proteins are compared in order to establish evolutionary relationships[5–7]. These proteins are used for this purpose due to their low intergenic sequence homology (20-30%) but high intragenic sequence homology (>85%)[1]. The second criterion is that viruses within the same genus must be able to reassort and produce viable progeny[5].

In 2011, a novel virus was isolated by Hause et al.[7] from nasal swabs collected from clinically ill pigs. Observation of the virus via electron microscopy revealed enveloped,

pleomorphic particles with dense projections on their surface, suggesting the virus belonged to the *Orthomyxoviridae* family. Enzyme assays demonstrated the virus lacked detectable neuraminidase activity but possessed O-acetylesterase, consistent with viruses in the ICV genus. Supporting this assertion was the discovery that the new virus had 7 genomic segments. As a result, the virus was provisionally named C/swine/Oklahoma/1334/2011 (C/OK). However, real-time reverse transcription PCR (qRT-PCR) and RT-PCR analyses were negative for IAV, IBV, and ICV strains[7].

In order to definitively classify C/OK into one of the influenza genera, the amino acid sequence of its PB1 protein was aligned to that of several human IAV, IBV, and ICVs[7]. C/OK was found to share 69-72% mean pairwise identity to ICVs. This level of identity is comparable to the level of homology observed between IAV and IBV PB1 proteins (61%) and is significantly lower than the high identity typically observed between viruses belonging to the same genus (reaching 90% in PB1s from intrasubtype IAVs). Alignment of PB1 sequences from C/OK and IAV and IBV demonstrated further diminished mean pairwise identity (39-41%). Similarly, when the amino acid sequence identity of the C/OK NP and M1 proteins were compared to other ICVs, only 38-41% identity was observed, well below the typical intragenic homology of >85%. When comparing overall amino acid identity, C/OK was found to be only 50% homologous to human ICV. Therefore, though these experiments suggested C/OK was most closely related to ICV, they also indicated that C/OK was distinct when compared to human ICVs.

To further clarify its taxonomic status, Hause et al.[5] conducted *in vitro* reassortment assays testing the ability of C/OK to productively reassort with human ICV. For these experiments, two human ICVs (C/Taylor/1947 and C/Johannesburg/66), C/OK, and a bovine

isolate closely related to C/OK (C/660) were selected. Following coinfection, plaques were picked and their full genomes sequenced to identify the presence of potential reassortant viruses. Though reassortant viruses were found following coinfection with either the two human viruses or the two non-human isolates, no reassortants were generated during coinfection with combinations of human and non-human viruses. This led the researchers to conclude that these non-human ICVs were genetically distinct from human ICVs. Furthermore, Hause et al. also demonstrated that C/OK could not be cross-recognized by polyclonal antisera generated in response to representative IAV, IBV, or ICV infections, suggesting that C/OK was also antigenically distinct from human ICV[5]. Together, the low sequence homology between the PB1, NP, and M1 proteins of C/OK and other human ICVs, in addition to C/OK's inability to reassort with human ICV and produce viable progeny led to the conclusion that C/OK meets neither criteria to be classified in the ICV genus. As a result, a fourth influenza genus in the *Orthomyxoviridae* family was proposed, influenza D virus (IDV)[5].

Cellular Tropism of Influenza D Virus

The evolutionary relationship of IDV to ICV is evident in their shared primary receptor, 9-O-acetyl-N-acetylneuraminic acid (Neu5,9Ac2). However, several studies have shown that IDV possesses a broader cellular tropism than ICV[6–8]. Structural modeling of IDV and ICV HEF proteins demonstrated that they share an enzymatic active site, leading to their consistency in receptor choice[7,8]. Despite this, modeling analysis also revealed variations in the receptor-binding pocket (RBP)[6,7], which is perhaps not surprising given the 53% sequence identity observed between D/OK (previously known as C/OK) and human ICV HEF proteins[7]. In the ICV HEF protein RBP, a negatively-charged D269 forms a salt bridge with the positively-charged K235, effectively closing off the end of the pocket. The equivalent amino acids in the

IDV HEF protein RBP cannot form this bridge, allowing for the generation of an open channel. The resulting open receptor binding cavity may allow IDV to recognize a larger repertoire of glycans which can then be used as cellular receptors[6,8]. Support for this theory has already come from research demonstrating the ability of IDV to recognize both Neu5,9Ac2 and 9-O-acetyl-N-glycolylneuraminic acid (which differs from Neu5,9Ac2 by the addition of an oxygen at the C5 position), whereas ICV strongly prefers Neu5,9Ac2[9]. Additionally, IDV lacks a glycosylation site at N233, located at the upper part of the RBP[6]. By removing this site, IDV HEF has increased access to the receptor, likely contributing to the broader cellular tropism of IDV[6]. Another possible influence on tropism is the IDV HEF protein's stronger binding capacity for Neu5,9Ac2 compared to the ICV HEF protein[8].

Recognition of Neu5,9Ac2 by IDV is the primary driver of cellular susceptibility to infection. O-acetylated sialic acids are distributed throughout the respiratory tract, however Neu5,9Ac2 is found specifically in the trachea (submucosal glands and apical surface) and lungs (alveolar pneumocytes and endothelia of vessels) of humans[6,8,10]. Neu5,9Ac2 has also been shown to be distributed in the tracheal epithelial cells of pigs, horses, dogs, mice, and Peking ducks, and in the lungs of ferrets, mice, and Peking ducks[10]. Consistent with these findings, IDV has been shown to replicate in the lower respiratory tract of pigs[11–13] and cattle[14]. Characterization of Neu5,9Ac2 distribution in the far upper respiratory tract, such as the nasal cavity, has yet to be conducted. However, IDV replication in the upper respiratory tract of pigs[7,11,12] and cattle[13] suggests the presence of Neu5,9Ac2 on these tissues as well. Overall, the tissue distribution of Neu5,9Ac2 within the respiratory tract and the cellular preference of IDV has yet to be fully elucidated.

Disease Presentation of Influenza D Virus

Clinical symptoms of influenza infections can range from mild, as seen typically in ICV infections, to severe and potentially life-threatening, which can occur in extreme cases of IAV or IBV infection[9]. Disease presentation because of influenza infection is thought to be tied to replication in the upper versus lower respiratory tract. Viruses capable of replicating at core body temperature (37˚C) are able to cause pathology in the lungs, potentially leading to severe disease[15]. This is in contrast to viruses whose infection is limited to the upper respiratory tract (32˚C), which have reduced or nonexistent replication in the lungs and thus do not induce serious illness[15].

Currently, the health implications of IDV infection in humans are unknown. The impact of IDV on non-human animals, however, has been investigated[9,16]. Typically, IDV infection in swine and cattle is associated with mild upper respiratory illness[7,17–19] associated with symptoms such as rhinitis and tracheitis[20], dry cough, nasal discharge, and depression[17]. IDV infection of the lower respiratory tract has been reported in cattle and swine as well, resulting in mild to moderate disease characterized by fever and lung lesions[12,18]. However, experimental hosts like guinea pigs[21] and ferrets[7] do not develop clinical signs of disease despite seroconverting and supporting viral replication.

It has also been speculated that IDV alone is not sufficient to cause severe disease, but may play a significant role in bovine respiratory disease (BRD)[22]. BRD is the most economically devastating affliction in the cattle industry, resulting in over a billion dollars in losses per year in the U.S. alone[22]. This disease is thought to result from the complex interplay between host, pathogens, and the environment. The leading theory suggests that stress induced by transport or other environmental factors followed by viral infection disrupts the airway epithelium, creating

opportunities for severe secondary infection of the respiratory tract by other viruses, bacteria, or parasites[22,23]. Several viruses, including bovine adenovirus 3 and bovine rhinitis A virus, have been implicated in the pathology associated with BRD[24]. IDV is also thought to play a role in these interactions due to its frequent detection in cattle presenting with BRD[5,22,24,25].

Route of Transmission

Facilitated by its ability to replicate in the upper and lower respiratory tract, the primary route of transmission for IDV is via direct contact[7,12,17]. In a study conducted by Lee et al.[12], all non-infected pigs commingled with IDV infected pigs seroconverted within 6 days, though no live virus was present in nasal swabs or bronchoalveolar lavage fluid samples[12]. These findings are in agreement with a study conducted in cattle where all naïve calves commingled with infected calves seroconverted within 6 days post exposure[17]. Of more zoonotic concern, IDV was able to transmit via direct contact between infected and non-infected ferrets[7]. Ferrets are commonly used as animal models for human respiratory diseases, particularly influenza, due to their similar lung physiology and ability to mimic the clinical presentation of human infection[26–28]. As a result, the ability of IDV to spread between ferrets suggests the potential for human transmission[7].

Other potential modes of transmission contributing to the spread of IDV are aerosols and respiratory droplets. In a study conducted by Salem et al.[18], non-infected calves separated by a three meter distance from directly inoculated calves began shedding IDV in nasal secretions ten days after the infected calves began to shed virus[18]. As part of the same study, IDV genome was detected in air samples collected from the inoculated group area, the space between the directly-inoculated and non-infected animals, and the non-infected animal area[18]. Additionally, in the ferret study conducted by Hause et al.[7], 1/3 of ferrets exposed to respiratory droplets

seroconverted, though none shed detectable virus. These results suggest that replication of IDV in the upper respiratory tract allows it to be spread by respiratory means in addition to direct contact.

Host Range and Geographic Distribution of Influenza D Virus

The ubiquitous presence of 9-O-acetyl sialic acid in the respiratory tract of animals provides IDV with a wide host and cell range. Currently IDV is known to naturally infect swine[11,29–31], wild boar[29], cattle[30], goats[31–33], sheep[30,32,33], camels[34,35], and horses[36] with virus or antibodies being observed in cattle and swine in the U.S. [6,7,25], Italy[11,37–39], U.K.[40], France[29,32,41], Ireland[42], China[31,43], Africa[34], Luxembourg[44], Turkey[45], Mexico[22], Japan[46,47], Argentina[48], and Canada[33]. Under experimental conditions mice[49], guinea pigs[21], and ferrets[7] have also been found to be susceptible to infection.

Despite being originally isolated from swine, infrequent isolation of IDV from pigs, low RT-PCR positivity to IDV in pigs, and multiple serological surveys demonstrating low seropositivity to IDV suggested that swine are not the primary host of the virus [5,7,11,30,32]. Alternatively, screening of bovine sera among U.S. cattle herds and newborn calves demonstrated 87.5%[50] and 94-98% [6,25,51] seropositivity respectively. Overall, the magnitude of IDV seropositivity seen in cattle is comparable to IAV seropositivity in waterfowl, the established reservoir for IAV[5]. Therefore, these high and widespread antibody titers in cattle suggest bovines are the natural host of IDV. This makes IDV the first influenza genus to use cattle as a reservoir[52,53].

Pandemic Potential of Influenza D Virus

The non-human primary host of IDV becomes significant when comparing the genera of influenza viruses. Unlike IDV, humans are the primary host and reservoir for IBV and ICV. In

addition, though IBV and ICV are capable of transmitting to animals, they do so rarely[1,4,7,11]. Similar to IDV and in contrast to IBV and ICV, IAV possesses a non-human natural host, waterfowl, and several maintenance hosts, including humans, swine, seals, mink, horses, dogs, birds, and others[6,54]. IAV is able to attain this diversity of host species because it has multiple genetically distinct subtypes including 18 HA and 11 NA subtypes, all combinations of which can be found in waterfowl[6,12]. Its wide host range and the vast genetic diversity generated by these multiple subtypes affords IAV its pandemic potential[7].

When two distinct IAVs infect the same cell, the 8 genomic segments of each virus are replicated simultaneously. In the process of packaging the genomic segments into new virions it is possible for reassortment to occur in which the genetic components of the first virus are shuffled with the second. As a result, a new virus is generated containing segments derived from both parent viruses. When this process leads to the generation of an IAV that can infect humans but encodes an HA subtype not normally seen in humans, it is called antigenic shift[6,55]. As a result of antigenic shift, it is possible to generate an animal virus capable of infecting humans. If the HA subtype encoded by this reassortant virus has not circulated in humans previously, the resulting influenza enters an immunologically naïve population with, by definition, an extremely high number of susceptible individuals[6]. It is in these scenarios that pandemics emerge, such as the 2009 H1N1 pandemic, which resulted from progressive reassortment between human, avian, North American swine, and Eurasian swine IAVs[56].

Though it is able to cause severe disease and is responsible for seasonal epidemics worldwide like IAV, IBV is not a pandemic threat. This is due to the fact that IBV is capable of antigenic drift but not antigenic shift[6,7]. Antigenic drift describes the steady accumulation of mutations in antibody binding sites over time, leading to a progressive loss of preexisting

immunity[6]. This constant level of change observed in both IAV and IBV is what requires the production of a new influenza vaccine every season. However unlike IAV, IBV is considered monosubtypic[7]. IBV exists in only two genetically and antigenically divergent lineages, Victoria and Yamagata. As a result, it does not possess the subtype diversity and potential for genetic reassortment necessary to afford it pandemic potential[7,12]. It is for this same reason that ICV is also not a pandemic threat. Although it exists in six genetically and antigenically distinct lineages, ICV is evolutionarily stable and is also monosubtypic[1,6,7,12]. Therefore, of the original three influenza genera, only IAV possesses the subtype diversity and zoonotic hosts necessary to impart it with the potential for zoonotic emergence and pandemic spread.

As of 2020, four lineages of IDV have been identified based on the sequence of their HEF protein. Represented by D/swine/Oklahoma/1334/2011 (D/OK), D/bovine/Oklahoma/660/2013 (D/660), D/bovine/Yamagata/10710/2016 (D/Yama2016), and D/bovine/Yamagata/1/2019 (D/Yama2019), the four lineages have been found to frequently reassort and some of these lineages co-circulate worldwide in both cattle and swine[6,53,57]. Though it is currently unknown whether multiple subtypes of IDV exist, its ability to infect and reassort within non-human maintenance hosts may allow the virus to act similarly to IAV. Adding to concerns about the virus, genomic analyses of IDVs isolated from a Mississippi cattle facility found evidence of antigenic drift along with active virus reassortment in cattle[57]. In the same study, it was shown that IDV seropositive cattle were not protected from experimental reinfection, potentially leading to the virus's widespread dissemination in animal populations[57]. Additionally, the evolutionary rate of IDV is 1.68×10^{-3} nucleotide substitutions per site per year in the HEF gene. This is significantly higher than ICV and on par with some subtypes of IAV (between $1–8 \times 10^{-3}$ nucleotide substitutions per site per year of the HA gene), suggesting that

IDV is not evolutionarily stable, unlike ICV[53]. Overall, non-human reservoirs, a wide natural host range, multiple reassorting lineages, and high substitution rate suggest that IDV could be of pandemic concern.

Influenza D Virus Infection of Humans

Influenza D viruses could pose a public health concern. Several serological surveys have been conducted to investigate the extent of IDV spillover into the human population. Serum samples collected from 316 individuals 60 years and older in Canada (i.e., Vancouver) and the U.S. (i.e., Connecticut) during the 2007-08 and 2008-09 influenza seasons demonstrated a seropositivity rate of 1.3%[7]. This low seroprevalence is in agreement with another study investigating 3300 human respiratory samples collected between 2006-08 from Edinburgh, Scotland, which detected no IDV by RT-PCR in any sample[58]. An investigation of occupational exposure to cattle in Florida during 2011-12, however, demonstrated a 97% seropositivity rate in cattle-exposed individuals versus 18% in non-cattle-exposed persons[59]. Though the small sample size (n=46: 35 cattle-exposed, 11 non-cattle-exposed) of this study should be taken into account, these results suggest that occupational zoonotic transmission of IDV may be taking place. A serologic study assessing the prevalence of IDV antibodies in the Italian population between 2005 and 2017 also suggested higher seroprevalence in the human population, though it showed an inconsistent increase in antibody titers[60]. In this study, antibodies to IDV were present in at least low levels (5.1% and 9.8%) every year. However, sharp increases (33.9-46.0%) were observed in years following epidemics of IDV in cattle and swine[60]. As a result, these findings suggest that spillover from an animal reservoir into the human population can occur but provide no evidence for IDV transmission within humans[60]. In summary, these studies suggest that

occupational contact with IDV-infected animals is the most probable route of human infection, although IDV is currently incapable of human-to-human transmission.

HYPOTHESIS

Due to its wide host range (e.g., cattle, pigs, and other domesticated animals) and high genome mutation rate, there is concern that IDV has the potential to serve as a zoonotic threat to humans. Prior to the isolation of IDV, IAV was the only influenza virus to have a non-human primary host, large subtype diversity, and pandemic potential[7]. While bovines are currently hypothesized to be the reservoir of IDV, the virus infects a wide range of species and serological surveys show the presence of antibodies that recognize IDV in human sera. Together, these findings illustrate that IDV can infect humans, but to date there is no evidence of human-to-human transmission[1,58–61]. Currently the cellular tropism and disease severity of IDV infection in humans are unknown. Additionally, it is unclear if IDV infects respiratory epithelial cells in both the upper and lower respiratory tract and to what extent physiological ranges of temperature (32˚C and 37˚C) impact cellular preference. In this study, I sought to characterize the ability of IDV to infect primary human nasal epithelial cells, determine its cellular tropism, and characterize the production of various innate immune factors in virus-infected cells. I also sought to determine how physiologically relevant temperature ranges (32˚C and 37˚C) could affect virus replication and induced cytokine/chemokine responses. I hypothesize that IDV will show limited replication in human nasal epithelial cell cultures and induce limited amounts of cytokines and chemokines after infection, explaining why significant IDV disease has not been reported in humans.

MATERIALS AND METHODS

Cell Lines

Madin Darby Canine Kidney (MDCK) cells were cultured in Dulbecco's Modified Eagle Medium (DMEM, Sigma-Aldrich) supplemented with 10% fetal bovine serum (FBS, Gibco Life Technologies), 100U/mL penicillin with 100µg/mL streptomycin (Quality Biological), and 2mM L-glutamine (Gibco Life Technologies) at 37˚C with 5% CO_2.

Human nasal epithelial cell (hNEC) cultures were isolated from the disease-free nasal tissue, collected during endoscopic sinus surgery mandated for disease-unrelated conditions. The cells were then differentiated at an air-liquid interface (ALI) in 24-well Falcon filter inserts (0.4-µM pore; 0.33 cm^2; Becton Dickinson) at 37˚C with 5% CO_2. ALI medium containing 1X ALI maintenance supplement (STEMCELL Technologies), 0.192 µg/mL hydrocortisone stock solution (STEMCELL Technologies), and 5 IU/mL 0.2% heparin solution (STEMCELL Technologies) was used as basolateral medium.

Viruses

Swine nasal swabs and nasal wipes were collected as part of the active influenza surveillance effort conducted by the Animal Influenza Ecology and Epidemiology Research Program at The Ohio State University, Department of Veterinary Preventive Medicine. Samples were collected during two agricultural exhibitions (11/5/2017 and 5/26/2018). At the time of sampling, none of the swine exhibited clinical signs of disease. In 2017, nasal swabs were collected from an agricultural exhibition in Kentucky where both pigs and cattle from multiple states across the U.S. were being shown, though the species were housed in different barns. In 2018, nasal wipes were collected at a swine-exclusive show in Ohio with pigs coming exclusively from Ohio. From these samples, researchers at The Ohio State University isolated

two viruses, D/swine/Kentucky/17TOSU1262/2017 – which they sequenced (consecutive GenBank accession numbers MK054178 to MK054184)[62], and D/swine/Ohio/18TOSU0287/2018. These two viruses – minimally passaged in MDCK cells – were provided to us along with six brain heart infusion broth (i.e., field) samples, two from 2017 and four from 2018, for attempted viral isolation. An ICV was selected from existing lab stocks to act as a comparison virus. Of the available viruses, influenza C/Ann Arbor/1/1950 was selected for its ability to replicate to measurable titers on MDCK cells.

IDV Isolation from Brain Heart Infusion Broth (BHIB) Samples

In order to isolate IDV virus from BHIB samples, 100% confluent MDCK cells in 3.5 cm^2 dishes were infected with 250µl of each BHIB sample diluted 1:1 in infection media (IM+NAT; DMEM, 0.3% Bovine Serum Albumin [BSA, Sigma], 100U/mL penicillin, 100µg/mL streptomycin, 2mM L-glutamine, and 5µg/mL N-acetyl trypsin [NAT; Sigma, St. Louis, MO]). The cells were infected at 37˚C with 5% CO_2 for 1 hour rocking every 10 minutes. After 1 hour, the inoculum was replaced with 1mL IM+NAT and the progression of cytopathic effect (CPE) monitored daily. Virus containing supernatant was collected when 70-90% CPE was achieved, approximately 5 days post infection. Infectious viral titer of the supernatant was then quantified using $TCID_{50}$ assays. Any supernatant found to contain virus was used to generate seed and working stocks.

50% Tissue Culture Infectious Dose ($TCID_{50}$) Assay

IDV $TCID_{50}$ assays were conducted using 96-well plates of 90-100% confluent MDCK cells. After the cells were washed twice with PBS+, ten-fold serial dilutions of each virus in IM were produced, and 20µL applied to 6 wells of cells. The plates were then incubated at 32˚C with 5% CO_2 for 6 days. The cells were then fixed with 4% formaldehyde in PBS overnight and

stained with Napthol Blue Black overnight. The resulting CPE was scored visually and the $TCID_{50}$ value for each sample was calculated using the Reed-Muench calculation[63].

Seed Stock and Working Stock

To produce IDV seed stocks, virus inoculum was generated by diluting virus or BHIB isolate to a multiplicity of infection (MOI) of 0.001 TCID50 units/cell in IM+NAT. Approximately 100% confluent T-150 (150 cm^2) flasks of MDCK cells were then washed twice with PBS+ (1x phosphate buffered saline [PBS] supplemented with calcium and magnesium) and infected with 5mL/flask of inoculum, rocking every 10 minutes for 1 hour at 32˚C with 5% CO_2. Each flask was then given 20mL of IM+NAT, incubated at 32˚C, and the progression of CPE monitored daily. Virus containing supernatant was collected when 70-90% CPE was achieved, approximately 4 days post infection. Infectious viral titer of the seed stocks was then determined using TCID50 assays. Working stocks were produced in the same fashion using the steed stock to generate the viral inoculum.

Plaque Assay

Plaque assays were performed in 6-well plates containing 90-100% confluent MDCK cells. The cells were washed twice with PBS+ then infected with 250µl of serial 10-fold dilutions of IDV in IM+NAT. The plates were then allowed to incubate at 32˚C with 5% CO_2 for 1 hour rocking every 10 minutes, after which the inoculum was aspirated and a layer of 1% agarose solution was added to each well. The 1% agarose was generated by adding 25mL of 2% agarose in water to 25 mL of 2x Modified Eagle Medium (Gibco Life Technologies) supplemented with 200U penicillin/mL, 200µg streptomycin/mL, 4mM L-glutamine, 0.2M HEPES (Gibco), and 5µg/mL NAT. After the agarose solidified, the plates were incubated at 32˚C for 4 days, fixed

with 4% formaldehyde (Fisher Chemical) in PBS overnight, then stained with Napthol Blue Black overnight.

To quantify plaque area, the wells and a ruler were imaged using a Nikon Fluorescence Dissection Microscope with an Olympus DP-70 color camera. The resulting pictures were uploaded to ImageJ (NIH), where the ruler image was used to set the reference scale of 1 cm and the Freehand Selector was used to trace the outline of each individual plaque, incorporating all cells showing CPE (including grey halos present around clear plaques). Plaque area measurements were then calculated by ImageJ and the resulting data transferred to GraphPad Prism 8 (GraphPad Software, San Diego, CA) for analysis and graphing.

Low MOI Growth Curves (GC)

MDCK

MDCK cells were seeded into 24-well plates and allowed to reach 100% confluence. After being washed twice with PBS+, the cells were infected with 100µL of virus diluted to a MOI of 0.001 in IM+NAT and set on a rocker for 1 hour at room temperature. The inoculum was then removed, the cells washed 2 times with PBS+, and 500µL of IM+NAT added to each well. The plates were then incubated at 32˚C or 37˚C with 5% CO_2 and samples collected at 1, 12, 24, 36, 48, 72, 96, 120, 144, and 168 hours post infection.

hNEC

Fully differentiated hNECs cultured on transwells in 24-well plates had their basolateral media collected and their apical surfaces washed three times by repeating the process of adding 100µL of IM with no NAT (IM-NAT), incubating for 10 minutes at 32˚C or 37˚C with 5% CO_2, then aspirating. The cells were then infected by adding 100µL of IDV diluted to a MOI of 0.1 in IM-NAT to the apical surface for 2 hours at 32˚C or 37˚C with 5% CO_2. Following infection, the

cells were washed three times with PBS- (PBS without calcium and magnesium) and then incubated at 32˚C or 37˚C with 5% CO_2. Apical samples were taken at 1, 12, 24, 36, 48, 72, 96, 120, 144, and 168 hours post infection by applying 100µL of IM-NAT to the apical surface, incubating at 32˚C or 37˚C for 10 minutes, removing the apical wash, and storing at -70˚C. Basolateral supernatants were collected and replaced every 48 hours. Infectious viral titer was then quantified using $TCID_{50}$ assays.

Deconvolution Microscopy of IDV Infection in hNECs

The cellular tropism of IDV was investigated through the use of deconvolution microscopy. The apical surface of differentiated hNEC cultures was washed three times by applying IM-NAT, incubating at 32˚C for 10 minutes, then aspirating the media. Fresh ALI was then added to the basolateral surface. The viruses were diluted to a MOI of 2 in IM-NAT then applied to the cells for 2 hours at 32˚C. Following this incubation period, the cells were washed three times with PBS- and were permitted to incubate at 32˚C for 16-18 hours.

After incubating overnight, the cells were fixed with 4% paraformaldehyde in PBS and the semipermeable membrane of the hNEC culture was cut in half. One half of the membrane was placed cell-side down in perm buffer (PBS- with 0.2% Triton X-100 [Sigma-Aldrich, St. Louis, MO]) followed by blocking buffer (5mL PBS-, 100uL normal goat serum [Sigma, St. Louis, MO], and 85uL 30% BSA). For detection of IDV infected cells, the hNECs were then incubated with rabbit polyclonal antibodies against swine D/OK IDV (Provided by the Feng Li Lab). Ciliated cells were identified using mouse monoclonal anti-tubulin Beta 4 (NBP2-00812, Novus Biologicals). Following a wash in wash buffer (PBS- and 0.2% Tween-20 [Sigma, St. Louis, MO]), the hNECs were secondarily stained with Alexa Fluor™ 488-labeled goat anti-rabbit IgG (H + L) (A11034, Life Technologies Corporation) and Alexa Fluor™ 555-labeled

goat anti-mouse IgG (H + L) (A21424, Life Technologies Corporation). The immunostained cultures were mounted on Superfrost®/Plus microscope slides (Fisherbrand) in ProLong™ Gold antifade reagent with DAPI (Invitrogen) and covered with 1oz. Premium Cover Glass (Fisher Scientific) coverslips. Z-stack images were then taken on a Zeiss AxioImager M2 microscope with attached Hamamatsu Digital Camera C10600 ORCA-R^2 using a step size of 0.5μm and the 40x/0.75 Ph2 objective. Images were deconvolved and cropped using the integrated Volocity software.

Interferon, Cytokine and Chemokine Measurements

Interferons, cytokines, and chemokines present in basolateral samples collected at 0, 48, 96, and 144 hours post infection during low MOI hNEC GCs were measured using the V-PLEX Human Chemokine Panel 1 (Eotaxin, MIP-1β, Eotaxin-3, TARC, IP-10, MIP-1α, IL-8, MCP-1, MDC, MCP-4) (Meso Scale Discovery) according to the manufacturers' instructions.

Statistical Analysis

Low MOI GCs were analyzed by mixed ANOVA with repeated measures followed by a Tukey's multiple comparisons test in GraphPad Prism 8. Plaque areas were analyzed by one-way ANOVA in GraphPad Prism 8. MSD data was processed in MSD DISCOVERY WORKBENCH 4.0 then analyzed for significant differences using GraphPad Prism 8 to conduct a mixed ANOVA (MANOVA) with repeated measures followed by a Tukey's multiple comparisons test.

RESULTS

Virus isolation from Brain Heart Infusion Broth (BHIB) samples

To reduce the risk of cross contamination between samples, BHIB samples provided by The Ohio State University were used to infect MDCK cells in individual 3.5 cm^2 dishes. Following inoculation, the dishes were monitored daily until 70-90% CPE was achieved. Most samples showed this level of CPE in 5 dpi (Figure 1). However, despite anti-bacterial supplements in the media, samples 17SW1268 and 18SW0287 showed evidence of bacterial and fungal contamination at 2 dpi at which point the dishes were discarded. Infectious viral titer of supernatants collected from the remaining dishes at 5 dpi were determined via TCID50 assay. Of the four samples that did not show contamination over the course of the experiment, only sample 17SW1262 had a titer above the assay's limit of detection (3.41×10^8 TCID50/mL; TCID50 assay LOD = 2.32×10^2 TCID50/mL). As a result, the virus isolated from sample 17SW1262 was designated D/swine/Kentucky/17SW1262/2017 (17SW) and was used to generate seed and working stocks for use in future experiments. I did not investigate what was causing the CPE in the other samples that did not yield infectious virus by TCID50 on MDCK cells.

IDV plaque assays conducted at 32˚C and 37˚C indicate a temperature sensitivity in the 2017, but not 2018, viruses

In order to evaluate the ability of 17SW, D/swine/Kentucky/17TOSU1262/2017 (17TOSU), and D/swine/Ohio/18TOSU0287/2018 (18TOSU) to infect and kill neighboring cells in a MDCK monolayer at temperatures representative of the upper and lower respiratory tract, plaque assays were conducted at 32˚C and 37˚C.

At 32˚C, all of the viruses generated clear plaques surrounded by a grey halo of dying cells (Figure 2B). Halos generated by 18TOSU infection were observed to be smaller than those

surrounding areas of clearance in 17TOSU and 17SW infections. Clearance of cells in the monolayer is indicative of the virus's ability to infect and kill cells at this temperature. Despite similarities in plaque morphology, variation in plaque area was observed between the three IDVs. Though the viruses displayed a wide range of plaque areas, 18TOSU was found to produce significantly larger plaques than 17TOSU (Figure 2A). This is evident when comparing the average plaque size for all the viruses (17SW: 0.913 ± 0.661 mm^2; 17TOSU: 0.824 ± 0578 mm^2; 18TOSU: 1.157 ± 0.741 mm^2). This suggests that 18TOSU was more capable of replicating and spreading to adjacent cells than 17TOSU, while 17SW was not significantly different from either.

Changing the temperature at which the assay was conducted had a large influence on plaque morphology. At 37˚C, only 18TOSU retained its ability to generate clear plaques in the MDCK monolayer. Neither 17TOSU nor 17SW were able to kill the cells they infected, resulting in diffuse plaques that were difficult to distinguish from the rest of the monolayer (Figure 3B). As a result, only plaques generated by 18TOSU were able to be quantified (Figure 3A). Also, the area of the plaques resulting from 18TOSU infection was dramatically impacted by temperature. Whereas 18TOSU's average plaque size was 1.079 ± 0.741 mm^2 at 32˚C, at 37˚C it was 4.437 ± 2.883 mm^2 (Figure 3A). This data indicates that 18TOSU is able to form clear, distinct plaques at both 32˚C and 37˚C, but the ability of 17TOSU and 17SW to form clear plaques was restricted to 32˚C.

Infectious viral growth kinetics on MDCK cells at 32˚C demonstrate efficient IDV replication in this cell type and temperature

The infectious growth kinetics of IDV infection were characterized by conducting multi-step growth curves on MDCK cells at 32˚C. Peak viral titer (approximately 8-9 LogTCID50/mL)

was achieved at 96 hpi for all viruses (Figure 4). After reaching peak titer, 18TOSU replication fell significantly below that of 17TOSU and 17SW. Thus, it can be concluded that all three IDV strains replicate efficiently at 32˚C, with the 2017 viruses reaching significantly higher titer than 18TOSU.

Infectious viral growth kinetics on hNEC cultures at 32˚C and 37˚C illustrate the ability of IDV to infect and replicate in a cell culture system representative of the human upper and lower respiratory tract

The ability of IDV to replicate in a physiologically relevant cell culture system was evaluated using multi-step growth curves on differentiated hNEC cultures at 32˚C and 37˚C (Figure 5A). At 32˚C, all three IDV strains reached peak viral titer at approximately 72 hpi and replicated to statistically significantly higher titers when compared to ICV, C/Ann Arbor/1/1950 (C/AA; Figure 5B). At 37˚C, 18TOSU and 17TOSU reached peak titer at 48 hpi and replicated to equivalently high titers (Figure 5C).

Though ICV is most closely related to IDV, several issues exist with using C/AA as a comparative virus. 17TOSU, 18TOSU, and 17SW are field isolates passaged minimally in cell culture so that they retain their natural infective ability. C/AA however is a virus isolated in 1950 that has been passaged extensively in cell culture, making it heavily cell culture adapted. Due to the mild disease presentation of ICV infection, surveillance for this genus of influenza virus is uncommon, making finding a field isolate of ICV challenging. For this reason, C/AA was not used in the 37˚C analysis of IDV replication. Additionally, 17SW and 17TOSU originated from the same field sample. The difference between these viruses is that 17TOSU was isolated and sequenced by The Ohio State University, whereas 17SW was isolated as part of this series of experiments and has not been sequenced. Due to extensive similarities in plaque morphology and

replication on MDCK and hNECs at 32˚C, it was assumed that 17TOSU and 17SW are identical and thus 17SW was not included in the 37˚C hNEC low MOI GCs.

The data demonstrated in Figure 5 indicate that IDV is capable of replicating to high titer in human primary nasal epithelial cells at temperatures mimicking the upper and lower respiratory tract, suggesting the potential to productively and efficiently infect humans *in vivo.* Additionally, high titer replication of influenza viruses at 37˚C is commonly associated with more severe disease. Thus, efficient replication of IDV at this temperature indicates a potential to cause disease in humans.

Deconvolution microscopy of IDV infected hNEC cultures indicates tropism for non-ciliated cells

The cellular tropism of IDV infection was investigated through deconvolution microscopy. hNEC cultures were stained to visualize the cellular localization of IDV and β-tubulin IV. β-tubulin IV is a cytoskeletal constituent of the microtubules present in cilia, therefore staining this component allows for the identification of ciliated cells. By carrying out deconvolution microscopy that allows several images to be taken in layers and resolved, fluorescently labeled objects at different depths within the sample are able to be viewed in focus simultaneously. Thus, allowing for visualization of both cilia on the surface of the cell and IDV replicating within the nucleus. If the anti-IDV and anti-β-tubulin IV staining overlaps, then it can be said that IDV preferentially infects ciliated cells. However, as seen in Figure 6, though all three IDVs appear to be infecting ciliated cells, the majority of ciliated cells in the hNEC culture are uninfected.

MSD analysis of the innate immune response induced by IDV compared to ICV infection of hNEC cultures at 32˚C

All three IDVs and a comparative ICV were used to infect hNEC cultures at 32˚C for up to 168 hpi with basolateral supernatants being collected at 0, 48, 96, and 144 hpi. Despite C/AA's heavy cell culture adaptation, infection with ICV is known to cause mild disease, making it an effective comparison for this analysis. Expression of 7 of the 10 factors evaluated differed between IDV and ICV infections. Of these factors only Eotaxin-3 and IP-10 secretion was upregulated, whereas IL-8, MCP-4, MDC, MIP-1α, and TARC expression was downregulated during IDV infection. Overall, differences in cytokine induction were consistent across all time points with the exception of Eotaxin-3 and IP-10 whose significance emerged at later timepoints (Eotaxin-3: 96 and 144 hpi, IP-10: 144 hpi). This consistent downregulation of several factors essential for the innate immune response to infection suggests either that IDV has a lesser disease presentation than ICV or that IDV has more enhanced immune evasion mechanisms than ICV.

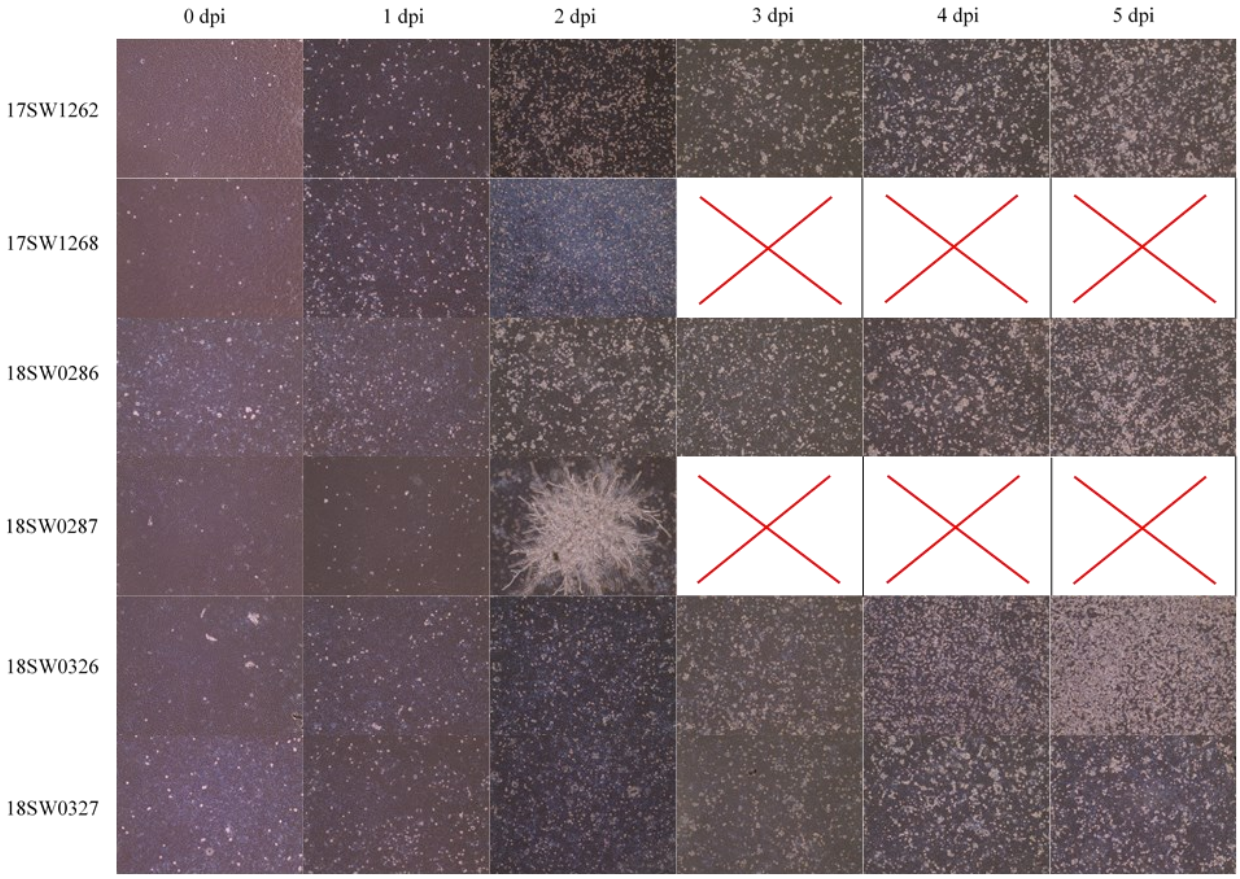

Figure 1. Virus Isolation from BHIB Samples. Individual 3.5 cm^2 dishes containing 100% confluent MDCK cells were infected with one BHIB sample each and monitored daily for CPE. Sample 17SW1268 showed signs of bacterial contamination at 2 dpi, as indicated by clouding in the supernatant. Fuzzy particles observed in sample 18SW0287 at 2 dpi suggested fungal contamination. As a result, the dishes containing 17SW1268 and 18SW0287 were discarded, thus no images of these samples are available for days 3-5 post infection, as is indicated by the red Xs. The remaining samples did not show any visible signs of contamination and thus were permitted to continue infecting up to 5 dpi at which point the supernatants were collected for titering. Images were taken on an EVOS Dissecting Microscope using the 4X objective.

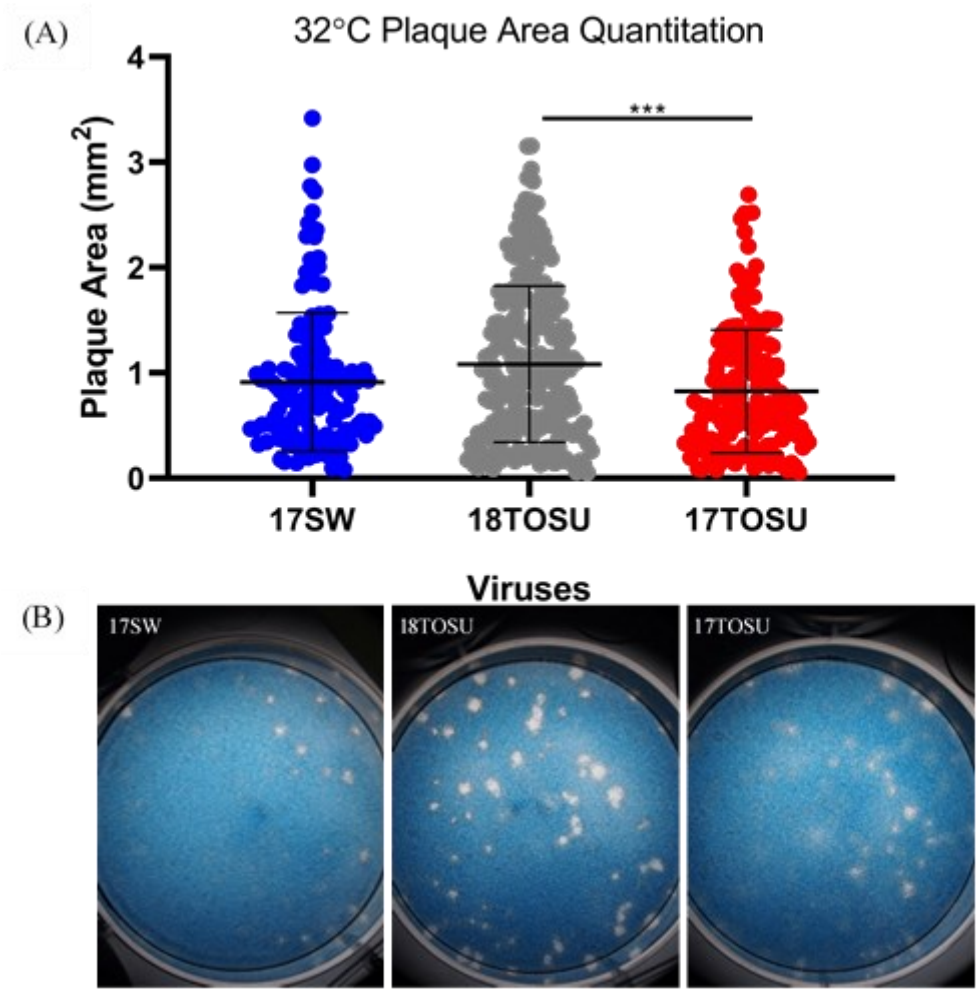

Figure 2. IDV Plaque Assay at 32˚C. Evaluating the ability of IDV to infect and kill adjacent cells in a MDCK monolayer through plaque area and morphology at 32˚C. (A) Plot of individual plaque area with lines representing mean and standard deviation. A minimum of 130 plaques coalesced from 3 independent experiments, each with 2 biological replicates, were quantified for each virus. Data points greater than two standard deviations from the mean were excluded as outliers. (B) Representative images of plaque morphology resulting from infection with 17SW, 18TOSU, and 17TOSU. Statistical significance was evaluated by one-way ANOVA (***$p<0.001$).

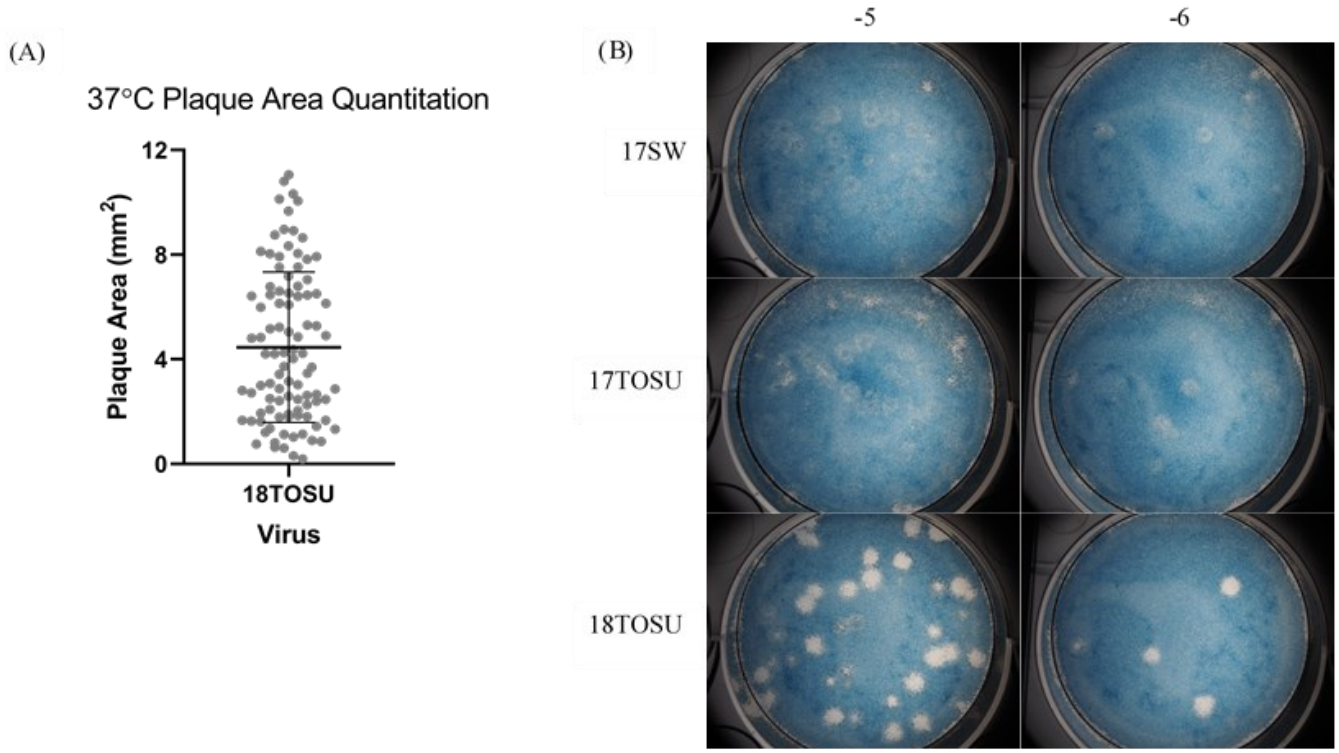

Figure 3. IDV Plaque Assay at 37˚C. Evaluating the ability of IDV to infect and kill adjacent cells in a MDCK monolayer through plaque area and morphology at 37˚C. (A) Plot of individual plaque area with lines representing mean and standard deviation. 97 plaques coalesced from 3 independent experiments, each with 2 biological replicates, were quantified for 18TOSU. (B) Representative images of plaque morphology resulting from infection with 17SW, 18TOSU, and 17TOSU. Numbers at the top of the image indicate dilution factor.

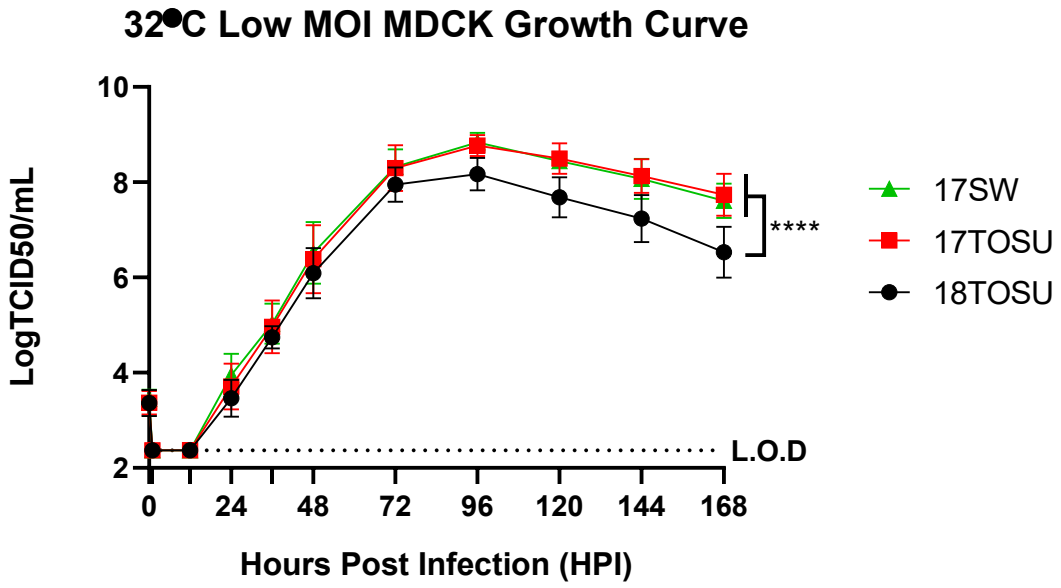

Figure 4. 32˚C IDV Low MOI MDCK GC. Multi-step growth curve performed on MDCK cells infected with a MOI of 0.01 at 32˚C. Statistical significance was measured using a MANOVA with repeated measures followed by a Tukey's post-test. Results are from 4 independent experiments, each with 3 biological replicates. ****$p<0.0001$. Limit of detection (L.O.D) = 2.37 logTCID50/mL.

(A)

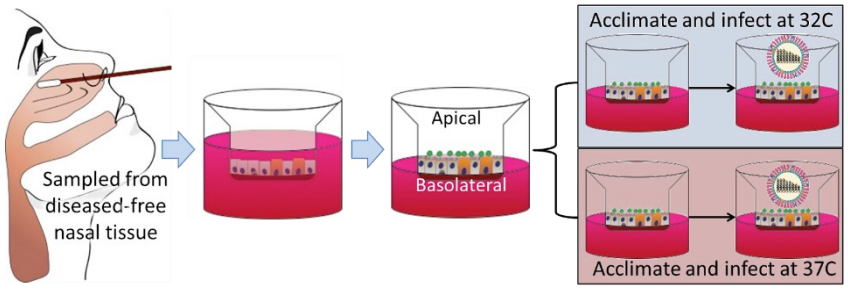

(B)

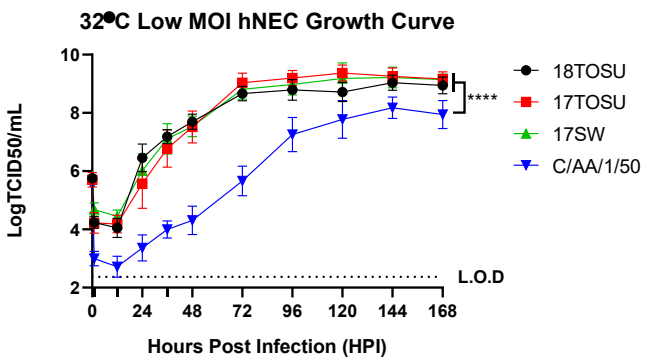

(C)

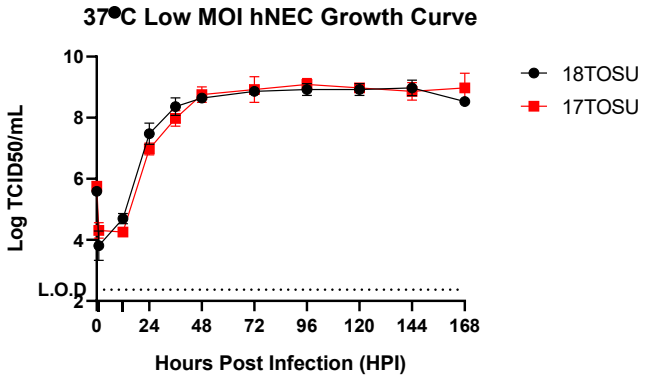

Figure 5. Low MOI hNEC GCs conducted at 32˚C and 37˚C demonstrate efficient replication of IDV in human cells. hNEC cultures provide an *in vivo* model representative of the human respiratory tract. (A) Image describing the hNEC workflow. Disease free nasal tissue collected during elective surgery is cultured at the air-liquid interface on transwell inserts. Following differentiation, the cells are acclimated to either 32˚C or 37˚C and then infected with the desired viruses. Samples were collected every 12 hours for the first 48 hours, then every 24 hours until 168 hpi. (B) Multi-step growth curve performed on differentiated hNEC cultures infected with a MOI of 0.1 at 32˚C. Results are from 3 independent experiments, each with 3 biological replicates. (C) Multi-step growth curve performed on differentiated hNEC cultures infected with a MOI of 0.1 at 37˚C. Results are from 1 independent experiment with 3 biological replicates. Statistical significance was measured using a MANOVA with repeated measures followed by a Tukey's post-test. ****p<0.0001. L.O.D = 2.37 log TCID50/mL.

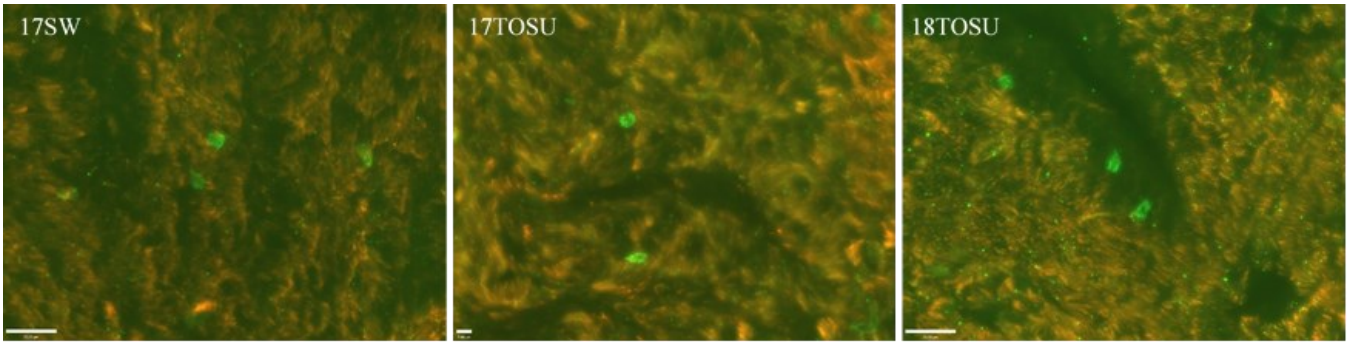

Figure 6. hNEC culture infected with 18TOSU imaged through deconvolution microscopy. These images were taken by a Zeiss AxioImager M2 microscope with attached Hamaumatsu camera. Anti-β-tubulin IV in the 555 channel fluoresces red, indicating the presence of cilia. Anti-C/OK in the 488 channel fluoresces green, indicating the presence of virus. Co-localization of β-tubulin and IDV was used as a qualitative evaluation of cellular tropism. Despite the cultures containing predominantly ciliated cells, indicated by the pervasive red staining, IDV was observed to infect a very limited number of cells. This suggests that the cellular tropism of IDV may be for non-ciliated cells.

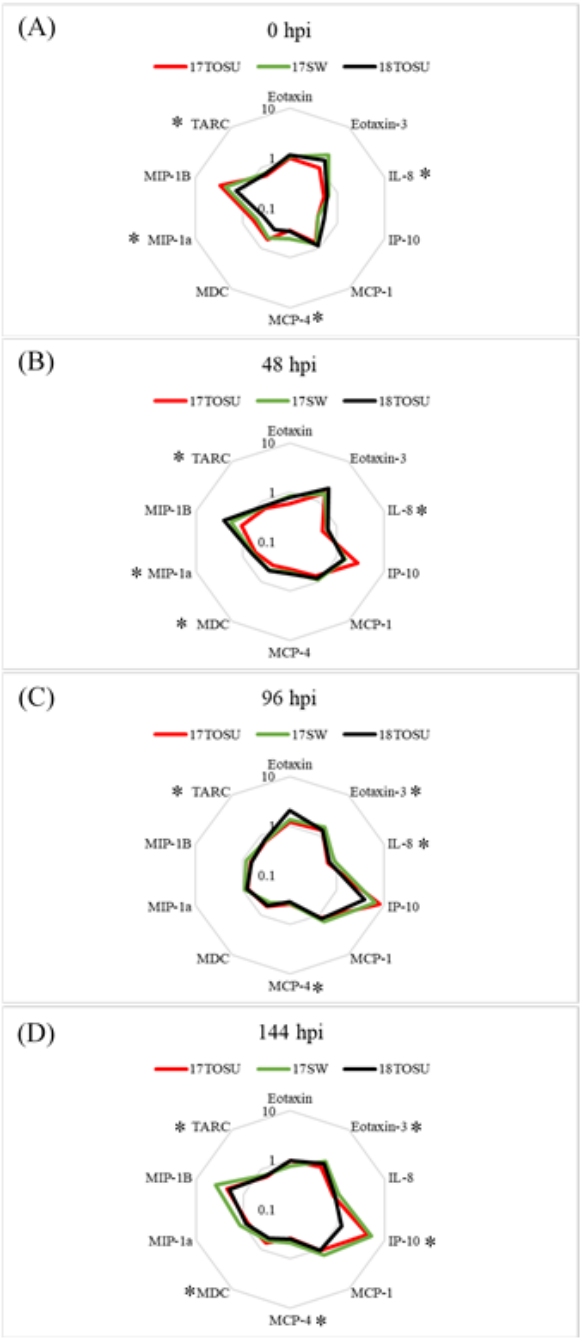

(E)

0 HPI	17TOSU	17SW	18TOSU
Eotaxin	ns	ns	ns
Eotaxin-3	ns	ns	ns
IL-8	ns	**	*
IP-10	ns	ns	ns
MCP-1	ns	ns	ns
MCP-4	*	*	*
MDC	ns	ns	ns
MIP-1α	ns	ns	*
MIP-1β	ns	ns	ns
TARC	ns	***	**

(F)

48 HPI	17TOSU	17SW	18TOSU
Eotaxin	ns	ns	ns
Eotaxin-3	ns	ns	ns
IL-8	***	**	**
IP-10	ns	ns	ns
MCP-1	ns	ns	ns
MCP-4	ns	ns	ns
MDC	**	**	****
MIP-1α	ns	*	ns
MIP-1β	ns	ns	ns
TARC	***	****	*

(G)

96 HPI	17TOSU	17SW	18TOSU
Eotaxin	ns	ns	ns
Eotaxin-3	**	ns	ns
IL-8	*	ns	*
IP-10	ns	ns	ns
MCP-1	ns	ns	ns
MCP-4	*	*	*
MDC	ns	**	ns
MIP-1α	ns	ns	ns
MIP-1β	ns	ns	ns
TARC	***	***	***

(H)

144 HPI	17TOSU	17SW	18TOSU
Eotaxin	ns	ns	ns
Eotaxin-3	ns	*	*
IL-8	ns	ns	ns
IP-10	ns	*	ns
MCP-1	ns	ns	ns
MCP-4	*	*	ns
MDC	ns	*	**
MIP-1α	ns	ns	ns
MIP-1β	ns	ns	ns
TARC	**	****	***

Figure 7. MSD analysis of the innate immune response to IDV infection at 32˚C. Basolateral supernatants collected at 0, 48, 96, and 144 hpi over the course of 32˚C low MOI hNEC GCs (Figure 5B) were evaluated via MSD assay. Results are from 3 independent experiments, each with 3 biological replicates. (A-D) Radar graphs illustrating fold change in cytokine expression induced by IDV infection compared to ICV infection. The Y-axis represents a logarithmic scale, therefore a value of 1 indicates no difference between 17TOSU, 17SW, or 18TOSU and C/AA. Values greater or lower than one indicates a difference from ICV. *= any significant difference between an IDV virus compared to C/Ann Arbor/1/1950. (A) MSD analysis of basolateral supernatants collected at the time of infection. (B) MSD analysis of basolateral supernatants

collected 48 hpi. (C) MSD analysis of basolateral supernatants collected 96 hpi. (D) MSD analysis of basolateral supernatants collected 144 hpi. (E-H) Tables detailing the level of significant difference between all three IDV viruses and C/AA for each timepoint post infection. Color indicates directionality of difference; blue indicates downregulation in comparison to C/AA and green indicates upregulation in comparison to C/AA. Statistical significance was measured using a MANOVA with repeated measures followed by a Tukey's post-test. *$p<0.05$, **$p<0.01$, ***$p<0.001$, ****$p<0.001$

DISCUSSION

Following the isolation of IDV in 2011, few studies have been conducted evaluating its potential as a human pathogen. Unlike its closest genetic relative ICV, IDV is neither exclusively a human pathogen nor evolutionarily stable. Instead, IDV possesses a bovine natural reservoir, a wide host range, multiple reassorting lineages, and a high substitution rate, all of which are more reminiscent of IAV, a virus known for zoonotic spillover and pandemic potential. These characteristics may cause IDV to be a threat to public health. Despite this evidence supporting the potential of IDV to infect humans, significant disease resulting from IDV infection has yet to be reported. In this study we sought to evaluate the zoonotic potential of IDV by evaluating its ability to replicate at physiologically relevant temperatures, investigating its cellular tropism, and measuring the innate immune response to infection as a proxy for disease presentation. Though we anticipated low levels of replication at 32˚C and 37˚C, we demonstrated that IDV readily infects and replicates to high titer at both temperatures in fully differentiated hNEC cultures. Additionally, we found significant differences in the cytokine and chemokine profiles induced by IDV versus ICV infection. Together, these results indicate that IDV is capable of replicating in the human nasal epithelial cells and may be capable of inducing disease. Therefore, we can conclude that IDV has the potential to pose a zoonotic threat to humans warranting further investigation.

Given that there are no reports of respiratory disease in humans caused by IDV infection, my results are surprising. Based on the robust replication observed in hNEC cultures, I would expect that both respiratory disease and transmission is possible in humans. This data suggests that increased surveillance for IDV in human populations – particularly humans in close contact with livestock – is warranted in order to determine the true disease potential of IDV infection.

While significant changes in cytokine and chemokine production were detected in IDV versus ICV infected hNEC cultures, the induction of most factors was decreased during IDV infection. This suggests that IDV either does not induce robust chemokine responses and therefore induces less immune mediated disease, or IDV possesses a very strong ability to inhibit host responses to infection. Given the significantly greater infectious virus production of IDV when compared to ICV in hNEC cultures, this reduced chemokine production was surprising. Typically, cytokine and chemokine induction in hNEC cultures is directly proportional to virus production, suggesting that the interaction of IDV with human nasal epithelial cells is considerably different when compared to ICV[64,65].

It is possible that severe disease after IDV infection in humans requires the presence of other respiratory pathogens, as seen in BRD. The lack of similar co-pathogens in humans may explain the lack of severe disease but our data on infectious virus titers produced in hNEC cultures would suggest prolonged virus shedding in humans is possible. Environmental factors such as temperature and humidity may be important barriers to IDV transmission in ways that are unique from IAV, IBV, and ICV.

MDCK cells are the gold standard for influenza virus isolation and propagation due to their surface expression of α2,6-sialic acid, α2,3-siaic acid, and Neu5,9Ac2, making them susceptible to infection by all genera of influenza[66,67]. However, the *in vivo* implications of results obtained using this immortalized cell line are limited. In contrast, hNEC cultures derived from disease free nasal tissue act as an *in vitro* surrogate model of the human respiratory tract, thus imbuing findings using these cells with greater clinical significance. As a result, we started our characterization of IDV growth kinetics on MDCK cells and used the outcomes to drive experiments in primary cell culture. In MDCKs, we found that IDV replicates to high titer at

32˚C. These results were mirrored in hNECs, where replication to high titer at 32˚C suggests IDV is able to actively infect the human upper respiratory tract, a finding widely supported by prior literature identifying IDV infection in the upper respiratory tract of pigs and cattle[7,11–13,17]. However, unlike past research suggesting that IDV titers decreased moving lower in the respiratory tract of cattle[6,17], low MOI hNEC GCs conducted at 37˚C revealed high titer replication, indicating that IDV has the potential to infect the lower respiratory tract and therefore may be capable of causing severe disease. These results are consistent with another *in vitro* study demonstrating efficient replication of IDV on primary cells at 37˚C[68].

Plaque assay analysis of the three IDV strains used in this study showed evidence of a temperature attenuation present in the 2017 viruses compared to the 2018 virus. Both 17SW and 17TOSU displayed vast changes in plaque morphology between 32˚C and 37˚C, becoming incapable of killing cells in an MDCK monolayer at higher temperature. In contrast, 18TOSU showed increased replication at 37˚C, as indicated by the larger plaque area, and maintained its ability to kill the cells it infected. This suggests that 18TOSU may possess enhanced replication in the lower respiratory tract as compared to 17SW and 17TOSU. However, when replication of the IDV strains was compared on hNEC cultures, 18TOSU did not demonstrate enhanced infection ability at 37˚C. This discrepancy in results is likely due to differences in cell type, in which the replication advantage of 18TOSU at 37˚C is present in MDCK cells but is not apparent in hNECs, suggesting that the temperature attenuation observed in the 2017 viruses on MDCKs would not hinder their ability to replicate in the lower respiratory tract *in vivo*.

Deconvolution microscopy qualitatively demonstrated that IDV does not preferentially infect ciliated cells. This is in disagreement with a previous study suggesting IDV shared ICV's tropism for ciliated cells[68]. Quantitative analysis, potentially by flow cytometry, is necessary to

definitively determine the cellular preference of IDV infection. Infections at higher MOIs and assessing cell tropism at later times post infection, for example at times of maximum infectious virus production, may also help clarify which cell types are primarily infected by IDV.

In summary, we demonstrated that IDV has the potential to efficiently infect and replicate within the upper and lower respiratory tract of humans. Due to its bovine natural reservoir, wide host range, multiple reassorting lineages, and high substitution rate, the ability of IDV to infect a primary cell culture system representative of the human respiratory tract could predict future zoonotic spillover and pandemic potential. As a result, our findings suggest that IDV warrants further investigation as a potential zoonotic pathogen and indicate that surveillance for this genus of influenza must be enhanced.

FUTURE DIRECTIONS

Though this study evaluated the replication kinetics of three IDV strains on MDCKs and hNEC cultures at 32˚C and 37˚C, additional experiments are needed to fully understand the influence of temperature on IDV infection. We failed to completely elucidate the cellular tropism of IDV infection. Therefore, deconvolution microscopy conducted either on hNEC cultures infected at higher MOIs or at later timepoints during maximum infectious virus production must be conducted. Alternatively, flow cytometry evaluating markers for all four cell types found in differentiated hNEC cultures and IDV could be carried out in order fully elucidate the cellular preference of IDV.

Additionally, our results demonstrated that cytokine and chemokine induction was significantly reduced during IDV infection compared to ICV infection. These findings can either be interpreted as IDV infection does not induce a robust innate immune response or that IDV is capable of inhibiting the production of chemokines in virus infected cells. Further studies clarifying this distinction will be important to determining if IDV is of lesser or greater zoonotic concern.

High viral titers achieved during IDV infection of hNEC cultures suggest severe disease and prolonged transmission in humans is possible, making the lack of reported infection in humans surprising. One potential explanation for this is that environmental factors not considered in our evaluation are essential to IDV transmission. Therefore, research investigating the impact of variables such as temperature and humidity on transmission must be carried out.

Finally, our results suggest that humans are susceptible to infection with IDV. A serological survey of sera from patients at Johns Hopkins Hospital could be carried out to

evaluate the presence of preexisting immunity to IDV in a non-cattle or swine exposed population to evaluate current risk of infection.

Appendix 1: SARS-CoV-2 Neutralizing Antibody Assays

INTRODUCTION

In December of 2019, SARS-CoV-2 emerged and quickly became a global pandemic. As a result, schools and research shut down across the globe. The Johns Hopkins Bloomberg School of Public Health was no exception. During this time, all non-SARS-CoV-2 related work was halted, including my thesis research on IDV. As our laboratory shifted to COVID-19 related research, I altered the focus of my work toward understanding antibody responses to SARS-CoV-2 infection by conducting neutralizing antibody (nAb) assays developed by our lab.

During primary infection with a virus or as a result of vaccination, virus-specific B cells are generated that produce anti-viral antibodies, most of which recognize the immunodominant S protein[69]. A proportion of these antibodies, particularly those specific for the RBD, are termed neutralizing antibodies (nAb)[69,70]. Through binding to the RBD, nAbs are able to block S protein interaction with the cellular receptor for SARS-CoV-2, angiotensin-converting enzyme II (ACE2)[71], rendering the virus incapable of attaching to target cells and thus preventing fusion with the cell membrane[69]. As a result, nAbs are considered the best correlate of protection against SARS-CoV-2 infection following natural infection or vaccination [69,72,73]. Therefore, research evaluating the presence and function of neutralizing antibodies is of critical importance. My contribution to the prodigious body of work surrounding SARS-CoV-2 has been to conduct nAb assays as part of larger projects outside of my lab answering a variety of different questions. Here I list the publications to which I have made a major contribution and detail my role in each. This is not an exhaustive list and only includes articles that have been published or are in preprint as of March 13th, 2021.

Benner et al. (2020). SARS-CoV-2 Antibody Avidity Responses in COVID-19 Patients and Convalescent Plasma Donors. ***The Journal of Infectious Diseases.*** **https://doi.org/10.1093/infdis/jiaa581** [74]

In this study, Benner et al.[74] strove to determine whether SARS-CoV-2-specific IgG titer and avidity are associated with neutralizing antibody titer. To accomplish this, plasma samples from 130 convalescent plasma donors and 16 hospitalized patients were used to conduct anti-SARS-CoV-2 S1- and N-specific IgG ELISAs, avidity assays, and nAb assays. The nAb assays I conducted acted as the gold standard to which the ELISA and avidity data were compared. Therefore, my work contributed significantly to the author's determination that anti-S and anti-N titers, in addition to anti-S avidity, but not anti-N avidity, are correlated to nAb titer. This led to the conclusion that avidity may be used in conjunction with other serologic testing to identify preferred individuals for convalescent plasma donation.

PubMed Hyperlink: https://pubmed.ncbi.nlm.nih.gov/32910175/

The Journal of Infectious Diseases
MAJOR ARTICLE

SARS-CoV-2 Antibody Avidity Responses in COVID-19 Patients and Convalescent Plasma Donors

Sarah E. Benner,[1] Eshan U. Patel,[1,2] Oliver Laeyendecker,[3,4] Andrew Pekosz,[5] Kirsten Littlefield,[5] Yolanda Eby,[1] Reinaldo E. Fernandez,[3] Jernelle Miller,[1] Charles S. Kirby,[1] Morgan Keruly,[4] Ethan Klock,[3] Owen R. Baker,[4] Haley A. Schmidt,[1] Ruchee Shrestha,[1] Imani Burgess,[1] Tania S. Bonny,[1] William Clarke,[1] Patrizio Caturegli,[1] David Sullivan,[3] Shmuel Shoham,[3] Thomas C. Quinn,[3,4] Evan M. Bloch,[1] Arturo Casadevall,[2,©] Aaron A. R. Tobian,[1,a] and Andrew D. Redd[2,4,a]

[1]Department of Pathology, Johns Hopkins School of Medicine, Baltimore, Maryland, USA, [2]Department of Epidemiology, Johns Hopkins Bloomberg School of Public Health, Baltimore, Maryland, USA, [3]Department of Medicine, Division of Infectious Diseases, Johns Hopkins School of Medicine, Baltimore, Maryland, USA, [4]Division of Intramural Research, National Institute of Allergy and Infectious Diseases, National Institutes of Health, Bethesda, Maryland, USA, and [5]W. Harry Feinstone Department of Molecular Microbiology and Immunology, Johns Hopkins Bloomberg School of Public Health, Baltimore, Maryland, USA

Background. Convalescent plasma therapy is a leading treatment for conferring temporary immunity to COVID-19–susceptible individuals or for use as post-exposure prophylaxis. However, not all recovered patients develop adequate antibody titers for donation and the relationship between avidity and neutralizing titers is currently not well understood.

Methods. SARS-CoV-2 anti-spike and anti-nucleocapsid IgG titers and avidity were measured in a longitudinal cohort of COVID-19 hospitalized patients (n = 16 individuals) and a cross-sectional sample of convalescent plasma donors (n = 130). Epidemiologic correlates of avidity were examined in donors by linear regression. The association of avidity and a high neutralizing titer (NT) were also assessed in donors using modified Poisson regression.

Results. Antibody avidity increased over duration of infection and remained elevated. In convalescent plasma donors, higher levels of anti-spike avidity were associated with older age, male sex, and hospitalization. Higher NTs had a stronger positive correlation with anti-spike IgG avidity (Spearman $\rho = 0.386$; $P < .001$) than with anti-nucleocapsid IgG avidity (Spearman $\rho = 0.211$; $P = .026$). Increasing levels of anti-spike IgG avidity were associated with high NT (≥160) (adjusted prevalence ratio = 1.58 [95% confidence interval = 1.19–2.12]), independent of age, sex, and hospitalization.

Conclusions. SARS-CoV-2 antibody avidity correlated with duration of infection and higher neutralizing titers, suggesting a potential alternative screening parameter for identifying optimal convalescent plasma donors.

Keywords. SARS-CoV-2; avidity; anti-spike; anti-nucleocapsid; convalescent plasma.

Severe acute respiratory syndrome coronavirus 2 (SARS-CoV-2), the cause of coronavirus disease (COVID-19), was declared a pandemic in early 2020 by the World Health Organization [1, 2]. As of 1 September 2020, there have been over 25 million confirmed COVID-19 cases and over 840 000 deaths [2, 3]. Symptoms of COVID-19 include cough, fever, fatigue, muscle pain, and shortness of breath, with hospitalized patients at higher risk of death [2–4].

Currently, there remains no prophylactic vaccine for SARS-CoV-2 infection and pharmaceutical therapeutics are limited. Convalescent plasma therapy is presently the best option to confer temporary immediate passive immunity for infection prevention or early treatment of individuals [5]. Historically, passive immune therapy has been used as post-exposure prophylaxis or hospital treatment for a variety of viral infections [5–9]. Observational studies have evaluated the use of convalescent plasma to treat COVID-19, suggesting both safety and efficacy, as reflected by shortened duration of hospitalizations and lower mortality (ie, as compared to nontransfused controls) [6–11].

Neutralizing antibodies in convalescent individuals are of major interest as they bind to various viral epitopes, inhibiting infectivity by blocking attachment or entry into host cells [12]. While the US Food and Drug Administration (FDA) initially did not require neutralizing antibody titer testing for potential convalescent plasma donors at the beginning of the pandemic, they recommended a target titer of > 1:320 for ideal donors if testing was available; this target titer was subsequently lowered [5, 13]. Additionally, 30% of recovered patients have low titers of SARS-CoV-2–specific neutralizing antibodies and > 5% have undetectable levels [5, 14]. Determinants of SARS-CoV-2 neutralizing antibody responses are largely unknown.

Of the 4 main structural SARS-CoV-2 proteins, spike (S1 subunit and receptor binding domain) and nucleocapsid proteins are the most immunogenic [15, 16]. In recent studies,

Received 22 July 2020; editorial decision 4 September 2020; accepted 8 September 2020; published online September 10, 2020.

[a]A. A. R. T. and A. D. R. are equal senior authors

Correspondence: Aaron A. R. Tobian, MD, PhD, Department of Pathology, School of Medicine, Johns Hopkins University, 600 N. Wolfe St, Carnegie Room 437, Baltimore, MD 21287 (atobian1@jhmi.edu).

The Journal of Infectious Diseases® 2020;222:1974–84

DOI: 10.1093/infdis/jiaa581

Bloch et al. (2021). ABO blood group and SARS-CoV-2 antibody response among convalescent plasma donors. *Vox Sanguinis.* https://doi.org/10.1111/vox.13070 [75]

In this paper, Blotch et al.[75] sought to determine the effects of ABO blood group on risk of SARS-CoV-2 infection and severity of COVID-19. In order to accomplish this, IgG and IgA were measured using the Euroimmun anti-SARS-COV-2 ELISA and nAb titers were measured using nAb assay for each of the ABO blood groups. By implementing my nAb assay data, the authors determined that nAb titers differed significantly by ABO group, individuals with blood group B possessed the highest nAb titers, followed by individuals with A, O and finally AB blood groups. This is in contrast to anti-S IgG or IgA which did not differ by blood group. Additionally, it was determined that significantly more individuals with blood group B had high nAb titers in comparison to blood group O. Therefore, my work contributed heavily to the conclusion that an individual's ABO blood group plays a role in susceptibility to SARS-CoV-2 infection and/or COVID-19 severity.

PubMed Hyperlink: https://pubmed.ncbi.nlm.nih.gov/33493365/

VoxSanguinis
The International Journal of Transfusion Medicine

Vox Sanguinis (2021)

DOI: 10.1111/vox.13070

ORIGINAL PAPER

ABO blood group and SARS-CoV-2 antibody response in a convalescent donor population

Evan M. Bloch,[1,†] Eshan U. Patel,[1,2,†] Christi Marshall,[1] Kirsten Littlefield,[3] Ruchika Goel,[1,4] Brenda J. Grossman,[5] Jeffrey L. Winters,[6] Ruchee Shrestha,[1] Imani Burgess,[1] Oliver Laeyendecker,[7,8] Shmuel Shoham,[8] David Sullivan,[3] Eric A. Gehrie,[1] Andrew D. Redd,[7,8] Thomas C. Quinn,[7,8] Arturo Casadevall,[3] Andrew Pekosz[3] & Aaron A. R. Tobian[1]

[1]Division of Transfusion Medicine, Department of Pathology, Johns Hopkins University, Baltimore, MD, USA
[2]Department of Epidemiology, Johns Hopkins Bloomberg School of Public Health, Baltimore, MD, USA
[3]Department of Molecular Microbiology and Immunology, Johns Hopkins Bloomberg School of Public Health, Baltimore, MD, USA
[4]Mississippi Valley Regional Blood Center, Springfield, IL, USA
[5]Department of Pathology and Immunology, Washington University School of Medicine in St. Louis, St. Louis, MO, USA
[6]Department of Laboratory Medicine and Pathology, Mayo Clinic, Rochester, MN, USA
[7]Division of Intramural Research, National Institute of Allergy and Infectious Diseases, National Institutes of Health, Baltimore, MD, USA
[8]Department of Infectious Diseases, Johns Hopkins University School of Medicine, Baltimore, MD, USA

Vox Sanguinis

Background and Objectives ABO blood group may affect risk of SARS-CoV-2 infection and/or severity of COVID-19. We sought to determine whether IgG, IgA and neutralizing antibody (nAb) to SARS-CoV-2 vary by ABO blood group.

Materials and Methods Among eligible convalescent plasma donors, ABO blood group was determined via agglutination of reagent A1 and B cells, IgA and IgG were quantified using the Euroimmun anti-SARS-CoV-2 ELISA, and nAb titres were quantified using a microneutralization assay. Differences in titre distribution were examined by ABO blood group using non-parametric Kruskal–Wallis tests. Adjusted prevalence ratios (aPR) of high nAb titre (≥1:160) were estimated by blood group using multivariable modified Poisson regression models that adjusted for age, sex, hospitalization status and time since SARS-CoV-2 diagnosis.

Results Of the 202 potential donors, 65 (32%) were blood group A, 39 (19%) were group B, 13 (6%) were group AB, and 85 (42%) were group O. Distribution of nAb titres significantly differed by ABO blood group, whereas there were no significant differences in anti-spike IgA or anti-spike IgG titres by ABO blood group. There were significantly more individuals with high nAb titre (≥1:160) among those with blood group B, compared with group O (aPR = 1·9 [95% CI = 1·1–3·3], $P = 0·029$). Fewer individuals had a high nAb titre among those with blood group A, compared with group B (aPR = 0·6 [95%CI = 0·4-1·0], $P = 0·053$).

Conclusion Eligible CCP donors with blood group B may have relatively higher neutralizing antibody titres. Additional studies evaluating ABO blood groups and antibody titres that incorporate COVID-19 severity are needed.

Received: 3 November 2020, revised 5 December 2020, accepted 16 December 2020

Key words: ABO group, convalescent plasma, COVID-19, SARS-CoV-2, titre.

Correspondence: Evan M. Bloch, Transfusion Medicine, Johns Hopkins University School of Medicine; Department of Pathology, Johns Hopkins Bloomberg School of Public Health (Joint appt. International Health), 600 N. Wolfe Street/Carnegie 446 D1, Baltimore, MD 21287, USA
E-mail: Ebloch2@jhmi.edu
[†]EMB and EUP contributed equally.

Introduction

Since its first description in China in December 2019, over 66 million cases of severe acute respiratory

Heaney et al. (2021) Comparative performance of multiplex salivary and commercially available serologic assays to detect SARS-CoV-2 IgG and neutralization titers. *MedRxiv*. https://doi.org/10.1101/2021.01.28.21250717 [76]

Collection of oral fluid for the detection of SARS-CoV-2 antibodies provides a non-invasive means of determining seropositivity. However, research comparing the performance of salivary tests with serologic and nAb assays is scarce. To address this, Heaney et al.[76] used paired saliva and plasma samples from 101 COVID-19 convalescent plasma donors to compare the ability of a multiplex salivary SARS-CoV-2 IgG assay recognizing antibodies to N, RBD, and S antigens to three enzyme immunoassays and nAb assays. By calculating positive (PPA) and negative percent agreement (NPA), overall percent agreement, and Cohen's kappa coefficient, the authors were able to evaluate the concordance between the assays. In comparison to the nAb assay, the PPA of the multiplex salivary assay ranged from 62.3% (N) to 96.6% (S) and the NPA varied between 18.8% (RBD) to 96.9% (S). Through conducting the nAb assays, I contributed to the author's conclusion that the multiplex salivary SARS-CoV-2 IgG assay performed comparably to commercially-available enzyme immunoassays and nAbs, suggesting that salivary tests could be used to screen the COVID-19 convalescent plasma donor pool, evaluate seroprevalence in the population, and monitor immune responses to vaccination.

PubMed Hyperlink: https://pubmed.ncbi.nlm.nih.gov/33532806/

Comparative performance of multiplex salivary and commercially available serologic assays to detect SARS-CoV-2 IgG and neutralization titers

Christopher D. Heaney[1,2,3], Nora Pisanic[1], Pranay R. Randad[1], Kate Kruczynski[1], Tyrone Howard[1], Xianming Zhu[4], Kirsten Littlefield[5], Eshan U. Patel[2,4], Ruchee Shrestha[4], Oliver Laeyendecker[6,8], Shmuel Shoham[6], David Sullivan[5,6], Kelly Gebo[2,6], Daniel Hanley[7], Andrew D. Redd[6,8], Thomas C. Quinn[6,8], Arturo Casadevall[5], Jonathan M. Zenilman[6], Andrew Pekosz[1,5], Evan M. Bloch[4*], Aaron A. R. Tobian[4,6*]

[1]Department of Environmental Health and Engineering, Bloomberg School of Public Health, Johns Hopkins University, Baltimore, MD, USA

[2]Department of Epidemiology, Bloomberg School of Public Health, Johns Hopkins University, Baltimore, MD, USA

[3]Department of International Health, Bloomberg School of Public Health, Johns Hopkins University, Baltimore, MD, USA

[4]Department of Pathology, Johns Hopkins University School of Medicine, Baltimore, MD, USA

[5]Department of Molecular Microbiology and Immunology, Bloomberg School of Public Health, Johns Hopkins University, Baltimore, MD, USA

[6]Department of Medicine, Johns Hopkins University School of Medicine, Baltimore, MD, USA

[7]Department of Neurology, Johns Hopkins University School of Medicine, Baltimore, MD, USA

[8]Division of Intramural Research, National Institute of Allergy and Infectious Diseases, National Institutes of Health, Baltimore MD

*Shared Senior Authors

Kared et al. (2021). SARS-CoV-2-specific CD8+ T cell responses in convalescent COVID-19 individuals. *The Journal of Clinical Investigation.* 10.1172/JCI145476[77]

Though nAb titer is thought to be the best correlate of protection against SARS-CoV-2 infection, studies have shown that individuals with low or undetectable nAb titers have been able to clear the virus[78], suggesting a greater characterization of the cellular immune response is warranted. Kared et al.[77] sought to elucidate the CD8+ T cell response in 30 SARS-CoV-2 convalescent individuals by using a multiplexed peptide-MHC tetramer approach to screen the full SARS-CoV-2 proteome. Using this approach, 408 SARS-CoV-2 candidate epitopes for CD8+ T cell recognition were identified allowing for identification and phenotypic characterization of virus-specific T cells ex vivo. When comparing expression of markers on SARS-CoV-2-specific T cells, consistent with T cell differentiation, to neutralizing antibody activity, a correlation was found suggesting higher marker expression was associated with stronger nAb activity. Thus, my nAb assays contributed to the author's conclusion that an effective nAb response following SARS-CoV-2 infection is associated with progressive differentiation of a broad and robust SARS-CoV-2 specific CD8+ T cell response.

PubMed Hyperlink: https://pubmed.ncbi.nlm.nih.gov/33427749/

The Journal of Clinical Investigation RESEARCH ARTICLE

SARS-CoV-2–specific CD8+ T cell responses in convalescent COVID-19 individuals

Hassen Kared,[1] Andrew D. Redd,[2,3] Evan M. Bloch,[4] Tania S. Bonny,[4] Hermi Sumatoh,[1] Faris Kairi,[1] Daniel Carbajo,[1] Brian Abel,[1] Evan W. Newell,[1,5] Maria P. Bettinotti,[4] Sarah E. Benner,[4] Eshan U. Patel,[4,6] Kirsten Littlefield,[7] Oliver Laeyendecker,[2,3] Shmuel Shoham,[3] David Sullivan,[7] Arturo Casadevall,[7] Andrew Pekosz,[7] Alessandra Nardin,[1] Michael Fehlings,[1] Aaron A.R. Tobian,[4] and Thomas C. Quinn[2,3]

[1]ImmunoScape, Singapore, Singapore. [2]Division of Intramural Research, National Institute of Allergy and Infectious Diseases, NIH, Bethesda, Maryland, USA. [3]Department of Medicine and [4]Department of Pathology, Johns Hopkins University School of Medicine, Baltimore, Maryland, USA. [5]Vaccine and Infectious Disease Division, Fred Hutchinson Cancer Research Center, Seattle, Washington, USA. [6]Department of Epidemiology and [7]Department of Molecular Microbiology and Immunology, Johns Hopkins Bloomberg School of Public Health, Baltimore, Maryland, USA.

Characterization of the T cell response in individuals who recover from severe acute respiratory syndrome coronavirus 2 (SARS-CoV-2) infection is critical to understanding its contribution to protective immunity. A multiplexed peptide-MHC tetramer approach was used to screen 408 SARS-CoV-2 candidate epitopes for CD8+ T cell recognition in a cross-sectional sample of 30 coronavirus disease 2019 convalescent individuals. T cells were evaluated using a 28-marker phenotypic panel, and findings were modelled against time from diagnosis and from humoral and inflammatory responses. There were 132 SARS-CoV-2–specific CD8+ T cell responses detected across 6 different HLAs, corresponding to 52 unique epitope reactivities. CD8+ T cell responses were detected in almost all convalescent individuals and were directed against several structural and nonstructural target epitopes from the entire SARS-CoV-2 proteome. A unique phenotype for SARS-CoV-2–specific T cells was observed that was distinct from other common virus-specific T cells detected in the same cross-sectional sample and characterized by early differentiation kinetics. Modelling demonstrated a coordinated and dynamic immune response characterized by a decrease in inflammation, increase in neutralizing antibody titer, and differentiation of a specific CD8+ T cell response. Overall, T cells exhibited distinct differentiation into stem cell and transitional memory states (subsets), which may be key to developing durable protection.

Introduction

The emergence of severe acute respiratory syndrome coronavirus 2 (SARS-CoV-2) rapidly evolved into a global pandemic. To date, over 75 million cases spanning 191 countries or territories have been reported, with more than 1.6 million deaths attributed to coronavirus disease 2019 (COVID-19). The clinical spectrum of SARS-CoV-2 infection is highly variable, spanning from asymptomatic or subclinical infection to severe or fatal disease (1, 2). Characterization of the immune response to SARS-CoV-2 is urgently needed in order to better inform more effective treatment strategies, including antivirals and rationally designed vaccines.

Antibody responses to SARS-CoV-2 have been shown to be heterogenous, whereby male sex, advanced age, and hospitalization status are associated with higher titers of antibodies (3). Low or even undetectable neutralizing antibodies in some individuals with rapid decline in circulating antibodies to SARS-CoV-2 after resolution of symptoms underscores the need to assess the role of the cellular immune response (4). Multiple studies suggest that T cells are important in the immune response against SARS-CoV-2, and may mediate long-term protection against the virus (5–9).

To date, studies that have evaluated SARS-CoV-2–specific T cells in convalescent individuals have focused on either characterization of responses to selected, well-defined SARS-CoV-2 epitopes, or broad assessment of T cell reactivity against overlapping peptide libraries (6–10). The assessment of the complete SARS-CoV-2 reactive T cell pool in the circulation remains challenging, and there is still much to be learned from capturing both the breadth (i.e., number of epitope-specific T cell responses recognized) and depth of T cell response (i.e., comprehensive phenotype) to natural SARS-CoV-2 infection. A study by Peng et al. indicated that the majority of those who recover from COVID-19 exhibit robust and broad SARS-CoV-2–specific T cell responses (8). Further, those who manifest mild symptoms displayed a greater proportion of polyfunctional CD8+ T cell responses compared with severely diseased cases, suggesting a role of CD8+ T cells in ameliorating disease severity.

Many current COVID-19 vaccine candidates primarily incorporate the SARS-CoV-2 spike protein to elicit humoral immunity (11–13). However, whether these approaches will induce long-term protection against SARS-CoV-2 infection or severe COVID-19 remain unknown. Gaining insight into the immune response that

Authorship note: HK, ADR, and EMB contributed equally to this work. MF, AART, and TCQ are co–senior authors.
Conflict of interest: HK, HS, FK, DC, BA, AN, EWN, and MF are shareholders or employees of ImmunoScape Pte Ltd. AN is on the Board of Directors of ImmunoScape Pte Ltd.

Submitted: October 26, 2020; **Accepted:** January 7, 2021; **Published:** March 1, 2021.
Reference information: *J Clin Invest*. 2021;131(5):e145476.
https://doi.org/10.1172/JCI145476.

Klein et al. (2020). Sex, age, and hospitalization drive antibody responses in a COVID-19 convalescent plasma donor population. *The Journal of Clinical Investigation.*[69]

COVID-19 CP therapy has been approved as a treatment for SARS-CoV-2 infection under the FDA's EUA[79]. However, titers of nAbs have been found to vary widely per individual, thus making some individuals better donors than others. In this study, Klein et al.[69] sought to identify characteristics associated with high nAb titers that would allow for the identification of preferred convalescent plasma donors. Age, sex, history of hospitalization for COVID-19, and time from infection to plasma collection were evaluated to determine their impact on different antibody responses via ELISA assays for anti-S protein domain S1-IgG, anti-S-IgG, and anti-S-RBD, in addition to nAb assays. Considering the nAb assay results alone, male sex, older age, and hospitalization for COVID-19 were indicative of a greater nAb response, whereas days since confirmation of infection was negatively associated with nAb area under the curve. In terms of effect size, hospitalization was found to be the most highly associated with the generation of nAbs. Therefore, by conducting nAb assays, I contributed to the conclusion that age, sex, and hospitalization status can be used to screen the CP donor pool for individuals that are most likely to have high levels of protective antibodies.

PubMed Hyperlink: https://pubmed.ncbi.nlm.nih.gov/32764200/

The Journal of Clinical Investigation RESEARCH ARTICLE

Sex, age, and hospitalization drive antibody responses in a COVID-19 convalescent plasma donor population

Sabra L. Klein,[1,2,3] Andrew Pekosz,[1,4] Han-Sol Park,[1] Rebecca L. Ursin,[2] Janna R. Shapiro,[3] Sarah E. Benner,[5] Kirsten Littlefield,[1] Swetha Kumar,[6] Harnish Mukesh Naik,[6] Michael J. Betenbaugh,[6] Ruchee Shrestha,[5] Annie A. Wu,[5] Robert M. Hughes,[5] Imani Burgess,[5] Patricio Caturegli,[5] Oliver Laeyendecker,[7,8] Thomas C. Quinn,[7,8] David Sullivan,[1] Shmuel Shoham,[7] Andrew D. Redd,[7,8] Evan M. Bloch,[5] Arturo Casadevall,[1] and Aaron A.R. Tobian [5]

[1]W. Harry Feinstone Department of Molecular Microbiology and Immunology, [2]Department of Biochemistry and Molecular Biology, [3]Department of International Health, and [4]Department of Environmental Health and Engineering, Johns Hopkins Bloomberg School of Public Health, Baltimore, Maryland, USA. [5]Department of Pathology, Johns Hopkins School of Medicine, Baltimore, Maryland, USA. [6]Advanced Mammalian Biomanufacturing Innovation Center, Department of Chemical and Biomolecular Engineering, Johns Hopkins University, Baltimore, Maryland, USA. [7]Department of Medicine, Division of Infectious Diseases, Johns Hopkins School of Medicine, Baltimore, Maryland, USA. [8]Division of Intramural Research, National Institute of Allergy and Infectious Diseases (NIAID), NIH, Bethesda, Maryland, USA.

Convalescent plasma is a leading treatment for coronavirus disease 2019 (COVID-19), but there is a paucity of data identifying its therapeutic efficacy. Among 126 potential convalescent plasma donors, the humoral immune response was evaluated using a severe acute respiratory syndrome coronavirus 2 (SARS–CoV-2) virus neutralization assay with Vero-E6-TMPRSS2 cells; a commercial IgG and IgA ELISA to detect the spike (S) protein S1 domain (EUROIMMUN); IgA, IgG, and IgM indirect ELISAs to detect the full-length S protein or S receptor–binding domain (S-RBD); and an IgG avidity assay. We used multiple linear regression and predictive models to assess the correlations between antibody responses and demographic and clinical characteristics. IgG titers were greater than either IgM or IgA titers for S1, full-length S, and S-RBD in the overall population. Of the 126 plasma samples, 101 (80%) had detectable neutralizing antibody (nAb) titers. Using nAb titers as the reference, the IgG ELISAs confirmed 95%–98% of the nAb-positive samples, but 20%–32% of the nAb-negative samples were still IgG ELISA positive. Male sex, older age, and hospitalization for COVID-19 were associated with increased antibody responses across the serological assays. There was substantial heterogeneity in the antibody response among potential convalescent plasma donors, but sex, age, and hospitalization emerged as factors that can be used to identify individuals with a high likelihood of having strong antiviral antibody responses.

Introduction

Severe acute respiratory syndrome coronavirus 2 (SARS–CoV-2), the causative agent of coronavirus disease 2019 (COVID-19), emerged in Wuhan, China, in December 2019. Following the rapid, global spread of SARS–CoV-2 in March 2020, COVID-19 was declared a pandemic. By October 2020, over 35 million cases were confirmed, spanning 188 countries or territories and accounting for over 1 million deaths (1). Preventive and treatment options are limited, of which antibody therapy (i.e., convalescent plasma collected from individuals after recovery from COVID-19) has emerged as a leading treatment for COVID-19 (2). Observational findings are encouraging, suggesting improved clinical outcomes in those who are transfused with COVID-19 convalescent plasma (CCP), including radiological resolution, a reduction in viral loads, and improved survival (3–8). Although 2 randomized trials assessing CCP in China and Europe were terminated early and underpowered, they did not find clinically significant differences between the study arms (6, 9). Nonetheless, there is a lack of standardization of units of CCP that are being transfused, in large part because of limited data correlating antibody assays with formal virus neutralization activity.

Antibody responses that target the immunodominant SARS–CoV-2 spike (S) protein — specifically, those that target the S protein receptor–binding domain (S-RBD) — are thought to be highly associated with virus neutralization by blocking the interaction between S-RBD and the virus receptor angiotensin-converting enzyme 2 (AEC2) (10). The SARS–CoV-2 S protein is a highly glycosylated, trimeric protein that requires proteolytic processing to become fusogenic and mediate virus-host membrane fusion (11, 12). The S-RBD domain is partially masked in the prefusion structure of S protein and must be converted to an "open" conformation for optimal binding of S to ACE2 (13). Neutralizing antibodies (nAbs) are of particular interest, because they prevent viral

Authorship note: SLK, EMB, AC, and AART are co-senior authors.
Conflict of interest: EMB reports receiving personal fees and nonfinancial support from Terumo BCT and personal fees and nonfinancial support from Grifols Diagnostic Solutions. EMB is a member of the United States FDA Blood Products Advisory Committee. Any views or opinions that are expressed in this manuscript are those of the authors, based on their own scientific expertise and professional judgment; they do not necessarily represent the views of either the Blood Products Advisory Committee or the formal position of the FDA, and also do not bind or otherwise obligate or commit either the advisory committee or the agency to the views expressed.

Submitted: July 7, 2020; **Accepted:** August 6, 2020; **Published:** October 19, 2020.
Reference information: *J Clin Invest.* 2020;130(11):6141–6150.
https://doi.org/10.1172/JCI142004.

Morgenlander et al. (2021). Antibody responses to endemic coronaviruses modulate COVID-19 convalescent plasma functionality. *The Journal of Clinical Investigation.* 10.1172/JCI146927[80]

Prior exposure to coronaviruses other than SARS-CoV-2 has been predicted to impact CP therapy effectiveness[81]. In this article, Morgenlander et al.[81] sought to evaluate the functionality of convalescent plasma and screen its reactivity across the genomes of SARS-CoV-2 and four endemic human coronaviruses. Functionality was defined as virus neutralization, antibody dependent cellular phagocytosis (ADCP), antibody dependent cellular cytotoxicity (ADCC), and antibody dependent complement deposition (ADCD) and an algorithm was used to deconvolve cross-reactivity between peptides. The nAb titer (NT), ADCP, ADCC, and ADCD of CP from 126 donors was evaluated and the cohort was divided into high, medium, and low NT groups. VirScan was then used to assess peptide epitopes targeted by each of the 126 samples across the genomes of SARS-CoV-2, all 4 HCoVs, SARS-CoV-1, MERS, and 3 bat-CoVs. Through the use of nAb assays, the authors were able to conclude that high polyclonality of SARS-CoV-2 antibodies was a predictor of high nAb titer and that high NT plasma and low NT plasma recognized mostly the same immunodominant epitopes, though high NT plasma did so at a higher frequency. Also, NT, ADCC, ADCP, and ADCD were found to be correlated, though individual epitopes had variable associations with the different functionalities. For example, antibodies that recognized the immunodominant RBD, fusion peptide, and S1/S2 cleavage site peptides were most likely to neutralize SARS-CoV-2, regardless of whether they were generated by SARS-CoV-2 or HCoV infection. Thus, my nAb assays contributed significantly to the conclusion that prior exposure to HCoVs likely impacts the antibody response to SARS-CoV-2 infection and the effectiveness of COVID-19 CP therapy.

PubMed Link: https://pubmed.ncbi.nlm.nih.gov/33571169/

JCI The Journal of Clinical Investigation

Antibody responses to endemic coronaviruses modulate COVID-19 convalescent plasma functionality

William R. Morgenlander, … , Aaron A.R. Tobian, H. Benjamin Larman

J Clin Invest. 2021. https://doi.org/10.1172/JCI146927.

Research In-Press Preview Immunology Infectious disease

Graphical abstract

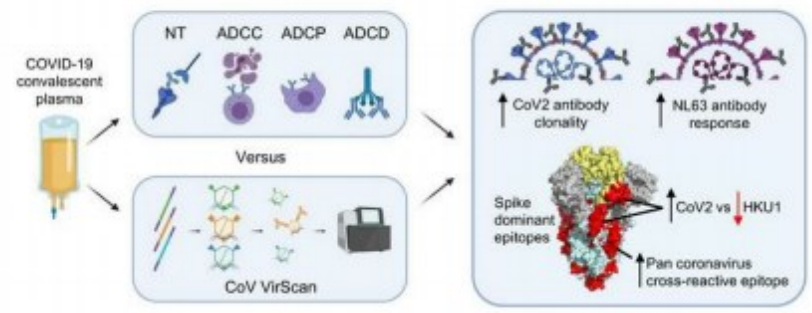

Ogega et al. (2021). Durable SARS-CoV02 B cell immunity after mild or severe disease. *The Journal of Clinical Investigation.* https://doi.org/10.1172/JCI145516[82]

One of the primary concerns following infection with or vaccination against SARS-CoV-2 is the potential for wanning immunity. Time dependent loss of SARS-CoV-2-sepcific antibodies could allow for reinfection or infection post-vaccination. To investigate the durability of the humoral immune response to SARS-CoV-2, Ogega et al.[82] performed multi-dimensional flow cytometric analyses of S-RBD-specific memory B cells (MBC) from patients with mild, moderate, and severe COVID-19 at approximately 54 days post symptom onset. nAb assays were conducted as part of this study to evaluate the possibility of waning nAb titers indicating a waning humoral response. By conducting the nAb assays, I helped in the determination that low nAb titers are not correlated with detection of S-RBD-specific class-switched MBC. Additionally, the publication concludes that S-RBD-specific non-class-switched B cells, S-RBD-specific class-switched antibody secreting cells, and/or S-RBD-specific class-switched MBC were detected in all the individuals studied, independent of nAb titer and severity of disease. These results allowed the authors to conclude that most SARS-CoV-2 infected people, even individuals with mild disease or low nAb titers, generate S-RBD-specific class-switched MBC, suggesting durable humoral immunity post recovery.

PubMed Link: https://pubmed.ncbi.nlm.nih.gov/33571162/

The Journal of Clinical Investigation RESEARCH ARTICLE

Durable SARS-CoV-2 B cell immunity after mild or severe disease

Clinton O. Ogega,[1] Nicole E. Skinner,[1] Paul W. Blair,[1] Han-Sol Park,[2] Kirsten Littlefield,[2] Abhinaya Ganesan,[2] Santosh Dhakal,[2] Pranay Ladiwala,[3] Annukka A.R. Antar,[1] Stuart C. Ray,[1] Michael J. Betenbaugh,[3] Andrew Pekosz,[2] Sabra L. Klein,[2] Yukari C. Manabe,[1] Andrea L. Cox,[1,2] and Justin R. Bailey[1]

[1]Division of Infectious Diseases, Department of Medicine, Johns Hopkins University School of Medicine, Baltimore, Maryland, USA. [2]W. Harry Feinstone Department of Molecular Microbiology and Immunology, The Johns Hopkins Bloomberg School of Public Health, Baltimore, Maryland, USA. [3]Advanced Mammalian Biomanufacturing Innovation Center, Department of Chemical and Biomolecular Engineering, Johns Hopkins University, Baltimore, Maryland, USA.

Multiple studies have shown loss of severe acute respiratory syndrome coronavirus 2–specific (SARS-CoV-2–specific) antibodies over time after infection, raising concern that humoral immunity against the virus is not durable. If immunity wanes quickly, millions of people may be at risk for reinfection after recovery from coronavirus disease 2019 (COVID-19). However, memory B cells (MBCs) could provide durable humoral immunity even if serum neutralizing antibody titers decline. We performed multidimensional flow cytometric analysis of S protein receptor binding domain–specific (S-RBD–specific) MBCs in cohorts of ambulatory patients with COVID-19 with mild disease ($n = 7$), and hospitalized patients with moderate to severe disease ($n = 7$), at a median of 54 days (range, 39–104 days) after symptom onset. We detected S-RBD–specific class-switched MBCs in 13 of 14 participants, failing only in the individual with the lowest plasma levels of anti–S-RBD IgG and neutralizing antibodies. Resting MBCs (rMBCs) made up the largest proportion of S-RBD–specific MBCs in both cohorts. FCRL5, a marker of functional memory on rMBCs, was more dramatically upregulated on S-RBD–specific rMBCs after mild infection than after severe infection. These data indicate that most SARS-CoV-2–infected individuals develop S-RBD–specific, class-switched rMBCs that resemble germinal center–derived B cells induced by effective vaccination against other pathogens, providing evidence for durable B cell–mediated immunity against SARS-CoV-2 after mild or severe disease.

Introduction

We are in the midst of an ongoing global pandemic caused by a novel coronavirus, severe acute respiratory syndrome coronavirus 2 (SARS-CoV-2). Coronavirus disease 2019 (COVID-19), the disease caused by SARS-CoV-2, can cause pulmonary inflammation, acute respiratory distress syndrome (ARDS), respiratory failure, and death. Despite the high morbidity and mortality caused by COVID-19, the majority of SARS-CoV-2–infected individuals recover and survive (1, 2). Following recovery, the durability of immunity against SARS-CoV-2 remains unclear. Durability of immunity is critical to mitigate the risk of reinfection for millions of people who have recovered or will recover from COVID-19.

After clearance of an infection or effective vaccination, phenotypically distinct B cell populations contribute to short- and long-term humoral immunity. Short-lived antibody-secreting cells (ASCs) in blood and secondary lymphoid organs release antibodies into the circulation for weeks to months. Durable humoral immunity (lasting months to years) is mediated by bone marrow–resident, long-lived ASCs and by memory B cells (MBCs), which rapidly proliferate and differentiate into ASCs in response to antigen rechallenge. Multiple studies have now demonstrated that serum antibody titers against SARS-CoV-2 wane and can even become undetectable after resolution of infection (3–6), likely reflecting a decline in short-lived ASC populations over time. Although other emerging reports have demonstrated more durable serum antibody responses (7–10), concerns remain that individuals who have recovered from COVID-19 may not maintain adequate immunity against reinfection. Individuals with mild COVID-19 disease generally mount lower titer antibody responses against the virus than those with severe disease (3, 10), raising particular concern that those who recover from mild infection are not protected against reinfection. If present and functional, MBCs could provide durable humoral immunity even after the loss of detectable serum antibody titers, as has been demonstrated after vaccination against viruses like hepatitis B (11, 12). However, Kaneko et al. showed a dramatic loss of germinal centers during acute COVID-19, raising concern that T cell–dependent, durable, class-switched SARS-CoV-2–specific MBC responses may not reliably develop after SARS-CoV-2 infection (13).

Little is known about the frequency and phenotype of SARS-CoV-2–specific MBCs that develop in response to either severe or mild infection. B cells specific for the SARS-CoV-2 Spike (S) protein have been isolated from individuals with very low antibody titers, but the relatively low frequency of these cells has thus far limited further characterization (14). We developed a highly sensitive and specific flow cytometry–based assay to quantitate circulating SARS-CoV-2 S protein receptor binding domain–specific

Conflict of interest: The authors have declared that no conflict of interest exists.

Submitted: October 28, 2020; **Accepted:** February 10, 2021; **Published:** April 1, 2021.
Reference information: *J Clin Invest.* 2021;131(7):e145516.
https://doi.org/10.1172/JCI145516.

Patel et al. (2021). Comparative performance of five commercially available serologic assays to detect antibodies to SARS-CoV-2 and identify individuals with high neutralizing titers. *The Journal of Clinical Microbiology*. DOI: 10.1128/JCM.02257-20[83]

Over the course of the pandemic several laboratory tests have arisen to detect anti-SARS-CoV-2 antibodies. In this study, Patel et al.[83] sought to evaluate the ability of five commercially available enzyme immunoassays (EIAs) to detect IgG or total anti-SARS-CoV-2 antibodies and nAbs. To do this, CP from 140 individuals were evaluating by all five EIAs and nAb assay. By comparing the EIAs to nAb assays, the authors determined that there was extensive variation in the EIAs ability to differentiate between low and high nAb titers in CP. As a result, my work contributed to the conclusion that discretion must be exercised when choosing which commercial EIA to use because not all are capable of identifying high nAb titers in convalescent individuals.

PubMed Link: https://pubmed.ncbi.nlm.nih.gov/33139419/

Journal of Clinical Microbiology®

VIROLOGY

Comparative Performance of Five Commercially Available Serologic Assays To Detect Antibodies to SARS-CoV-2 and Identify Individuals with High Neutralizing Titers

Eshan U. Patel,[a,b] Evan M. Bloch,[a] William Clarke,[a] Yu-Hsiang Hsieh,[c] Denali Boon,[d] Yolanda Eby,[a] Reinaldo E. Fernandez,[e] Owen R. Baker,[f] Morgan Keruly,[e] Charles S. Kirby,[a] Ethan Klock,[e] Kirsten Littlefield,[g] Jernelle Miller,[a] Haley A. Schmidt,[a] Philip Sullivan,[a] Estelle Piwowar-Manning,[a] Ruchee Shrestha,[a] Andrew D. Redd,[a,f] Richard E. Rothman,[c] David Sullivan,[g] Shmuel Shoham,[e] Arturo Casadevall,[g] Thomas C. Quinn,[e,f] Andrew Pekosz,[g] Aaron A. R. Tobian,[a,e] Oliver Laeyendecker[a,f]

[a]Department of Pathology, Johns Hopkins University School of Medicine, Baltimore, Maryland, USA
[b]Department of Epidemiology, Johns Hopkins Bloomberg School of Public Health, Baltimore, Maryland, USA
[c]Department of Emergency Medicine, Johns Hopkins University School of Medicine, Baltimore, Maryland, USA
[d]Department of Mental Health, Johns Hopkins Bloomberg School of Public Health, Baltimore, Maryland, USA
[e]Department of Medicine, Johns Hopkins University School of Medicine, Baltimore, Maryland, USA
[f]Division of Intramural Research, National Institute of Allergy and Infectious Diseases, National Institutes of Health, Baltimore, Maryland, USA
[g]Department of Molecular Microbiology and Immunology, Johns Hopkins Bloomberg School of Public Health, Baltimore, Maryland, USA

Aaron A. R. Tobian and Oliver Laeyendecker contributed equally to this article and are co-senior authors.

ABSTRACT Accurate serological assays to detect antibodies to severe acute respiratory syndrome coronavirus 2 (SARS-CoV-2) are needed to characterize the epidemiology of SARS-CoV-2 infection and identify potential candidates for coronavirus disease 2019 (COVID-19) convalescent plasma (CCP) donation. This study compared the performances of commercial enzyme immunoassays (EIAs) with respect to detection of IgG or total antibodies to SARS-CoV-2 and neutralizing antibodies (nAbs). The diagnostic accuracy of five commercially available EIAs (Abbott, Euroimmun, EDI, ImmunoDiagnostics, and Roche) for detection of IgG or total antibodies to SARS-CoV-2 was evaluated using cross-sectional samples from potential CCP donors who had prior molecular confirmation of SARS-CoV-2 infection ($n = 214$) and samples from prepandemic emergency department patients without SARS-CoV-2 infection ($n = 1,099$). Of the 214 potential CCP donors, all were sampled >14 days since symptom onset and only a minority ($n = 16$ [7.5%]) had been hospitalized due to COVID-19; 140 potential CCP donors were tested by all five EIAs and a microneutralization assay. Performed according to the protocols of the manufacturers to detect IgG or total antibodies to SARS-CoV-2, the sensitivity of each EIA ranged from 76.4% to 93.9%, and the specificity of each EIA ranged from 87.0% to 99.6%. Using a nAb titer cutoff value of ≥160 as the reference representing a positive test result ($n = 140$ CCP donors), the empirical area under the receiver operating curve for each EIA ranged from 0.66 (Roche) to 0.90 (Euroimmun). Commercial EIAs with high diagnostic accuracy to detect SARS-CoV-2 antibodies did not necessarily have high diagnostic accuracy to detect high nAb titers. Some but not all commercial EIAs may be useful in the identification of individuals with high nAb titers among convalescent individuals.

KEYWORDS COVID-19, SARS-CoV-2, serologic assays, neutralizing titers, convalescent plasma

Globally, as of October 2020, there were over 38.5 million reported cases of infection by severe acute respiratory syndrome coronavirus 2 (SARS-CoV-2), which causes coronavirus disease 2019 (COVID-19) disease (1). Surveillance based on case reporting

Citation Patel EU, Bloch EM, Clarke W, Hsieh Y-H, Boon D, Eby Y, Fernandez RE, Baker OR, Keruly M, Kirby CS, Klock E, Littlefield K, Miller J, Schmidt HA, Sullivan P, Piwowar-Manning E, Shrestha R, Redd AD, Rothman RE, Sullivan D, Shoham S, Casadevall A, Quinn TC, Pekosz A, Tobian AAR, Laeyendecker O. 2021. Comparative performance of five commercially available serologic assays to detect antibodies to SARS-CoV-2 and identify individuals with high neutralizing titers. J Clin Microbiol 59:e02257-20. https://doi.org/10.1128/JCM.02257-20.

Editor Michael J. Loeffelholz, Cepheid

Address correspondence to Oliver Laeyendecker, olaeyen1@jhmi.edu.

Received 28 August 2020
Returned for modification 14 September 2020
Accepted 29 October 2020
Accepted manuscript posted online 2 November 2020
Published 21 January 2021

Appendix 2: D614G Mutation of SARS-CoV-2

INTRODUCTION

On December 29, 2019, four patients presenting with pneumonia of unknown etiology were admitted to a hospital in Wuhan, Hubei Province, China [84]. Epidemiologic investigation revealed that the cases were associated with the Hunan Seafood Wholesale Market [84,85]. Due to the market's array of meats and live animals, a zoonotic source of the pathogen was suspected [84,86]. Additional cases reported on December 31st linked to the same market strengthened these suspicions [87]. However, subsequent epidemiological investigation into the increasing number of cases demonstrated that only 2% of patients interacted with wildlife directly, whereas over 75% were residents, visitors, or contacts associated with Wuhan[88,89]. This suggested potential human-to-human transmission[88,89]. Within a week of the first cases being reported, the etiologic agent of coronavirus disease 2019 (COVID-19) was isolated and determined to be a novel coronavirus, severe acute respiratory syndrome coronavirus 2 (SARS-CoV-2) [85,90]. By the 13th of January the first case outside of China occurred, opening the floodgates for an outpouring of international spread effecting countries in all six WHO regions [87,91]. On March 11th, 2020 the WHO officially declared the SARS-CoV-2 outbreak a global pandemic [92]. One year after the original four cases were reported, SARS-CoV-2 is now responsible for 128,540,982 confirmed cases and 2,808,308 deaths globally (as of March 31st, 2021)[93].

Introduction to SARS-CoV-2

SARS-CoV-2 is a non-segmented, positive sense, single-stranded RNA virus belonging to the *Betacoronavirus* genus within the *Coronavirinae* subfamily of the family *Coronaviridae* [89,94]. Within the *Coronavirinae* subfamily there are four genera, *Alphacoronaviruses* and *Betacoronaviruses*, which primarily infect mammals, and *Gammacoronaviruses* and

Deltacoronaviruses, which primarily infect birds [95]. Only seven coronaviruses have been known to infect humans, two are *Alphacoronaviruses*, HCoV-NL63 and HCoV-229E, and the remaining five are *Betacoronaviruses,* including HCoV-OC43, HCoV-HKU1, SARS-CoV, MERS-CoV, and SARS-CoV-2 [89]. Of these *Betacoronaviruses,* only SARS-CoV, MERS-CoV, and SARS-CoV-2 are capable of inducing fatal disease [96,97].

Lifecycle of SARS-CoV-2

The genome of SARS-CoV-2 encodes 6 open reading frames (ORFs) that generate 16 nonstructural proteins which comprise the replicase complex, 9 accessory proteins, and four structural proteins which include spike (S), envelope, membrane, and nucleocapsid[98–101]. Of these proteins, S mediates cellular entry, however it is initially generated in an inactive form. In order to be capable of mediating fusion, S must be proteolytically cleaved at the S1/S2 polybasic cleavage site into its subunits, S1 and S2[98,100,101]. Once cleaved by cellular or viral proteases, the S protein becomes fusogenic and its subunits take on unique functions. The S1 fragment possesses the receptor binding domain (RBD) which it uses to recognize and bind to the receptor, angiotensin-converting enzyme II (ACE2), on the surface of a susceptible cell[100,101]. Following interaction with ACE2, the virus is taken up into the cell within an endosome[98]. There the S2 fragment is cleaved again into S2', exposing a hydrophobic fusion peptide that mediates fusion between the viral envelope and the endosomal membrane[98,100,101]. Fusion between the membranes allows the viral genome to be released into the cytoplasm of the cell[98]. Due to the fact that the viral genome is a 5'-capped, positive sense RNA molecule it can be translated immediately into protein upon entry[99]. The first ORFs to be translated are ORF1a and 1b resulting in a polyprotein that is cleaved by a viral protease into individual proteins, some of which comprise the RNA-dependent RNA polymerase (RdRp) complex responsible for

replicating the viral genome. Once assembled, the RdRp reforms the endoplasmic reticulum into double-membrane vesicles which are used as factories for replication of the genome and generation of subgenomic RNAs which code for the viral structural and accessory proteins[98,101]. Following translation, the structural proteins are inserted into the endoplasmic reticulum-Golgi intermediate compartment where virion assembly takes place. The newly produced virions are then released at the plasma membrane via exocytosis[98,101].

Origin and Phylogenetic Characterization of SARS-CoV-2

Prior to the SARS-CoV-2 pandemic, SARS-CoV and MERS-CoV were the only known highly pathogenic coronaviruses. Though marked by higher case numbers and lower mortality, SARS-CoV-2 shows similarities in its path to emergence. From 2002 to 2003, SARS-CoV caused 8096 cases and 774 deaths (CFR = 9.6%), impacting 33 countries across the globe [102]. Serological analysis of pandemic SARS-CoV isolates demonstrated a 87-92% sequence identity to bat SARS-CoV, suggesting bats were the natural reservoir of the virus[103]. In addition, civet cats and raccoon dogs have been implicated as intermediate hosts during the SARS-CoV outbreak due to similarities in viral sequences infecting these species[97,104]. Middle East respiratory syndrome coronavirus (MERS-CoV) caused 2229 cases across 27 countries resulting in 791 deaths (CFR = 35.5%) between 2012 and 2018[105]. Similar to SARS-CoV, MERS-CoV has been shown to originate in bats and use an intermediate host, dromedary camels, for spillover into the human population[106].

In comparison to these highly pathogenic coronaviruses, the symptoms associated with SARS-CoV-2 are milder and its transmission between humans is more efficient. As a result, SARS-CoV-2 has caused tens of millions of cases but has a mortality rate of approximately 3.4%[97]. Phylogenetically, SARS-CoV-2 shares only ~80% sequence identity with SARS-CoV

and ~50% with MERS-CoV [107]. However, similar to the pattern of emergence seen in SARS-CoV and MERS-CoV, several studies have demonstrated that SARS-CoV-2 shares high sequence identity with bat coronaviruses, suggesting that bats are the probable species of origin [71,89,107–110]. Though bats are considered the source of the outbreak, at the time of the pandemic bats were hibernating and no bats were sold at the Hunan Seafood Wholesale Market, suggesting an intermediate host would be necessary to initiate human transmission [86]. Multiple studies have shown high sequence similarity (85.5-92.4%) between SARS-CoV-2 and Pangolin-CoV, suggesting that pangolins are a natural reservoir and potential intermediate host for SARS-CoV-2[89,109,111,112].

Cellular Tropism of SARS-CoV-2

SARS-CoV-2's broad cellular tropism may be responsible for the discrepancy between its prodigious case numbers and the comparatively smaller impact of SARS-CoV and MERS-CoV [98]. SARS-CoV-2 and SARS-CoV share the same functional receptor, angiotensin-converting enzyme II (ACE2)[71]. Important to the evolution of SARS-CoV-2, Zhou et al. demonstrated that the virus is able to use ACE2 from Chinese horseshoe bats, civets, and pigs for entry into cells[71]. However, alterations within the RBD of the SARS-CoV-2 S protein permit it to make additional contacts with ACE2, allowing it to bind with 10 times greater strength than SARS-CoV [113,114]. In addition, SARS-CoV-2 possesses a unique furin cleavage site, a RRAR insertion at the S1/S2 cleavage site in the S protein[98]. This may increase the virus's infectivity by making the S protein more susceptible to cleavage into its fusogenic form[98]. One cellular protease in particular has been shown to be responsible for coronavirus S protein priming, transmembrane protease serine 2 (TMPRSS2), though infection of cells lacking TMPRSS2 can be achieved in the presence of another cellular enzyme, cathepsin L [115]. However, due to SARS-

CoV-2's unique RRAR insertion, S can be precleaved into S1/S2 by furin, thus reducing the virus's dependence on cellular proteases and enhancing its fusogenic capabilities[98,114]. This enhanced affinity for ACE2 and enzyme promiscuity at the S1/S2 cleavage site are thought to contribute to the broad cellular tropism of SARS-CoV-2.

Upon entry into the respiratory tract, cellular susceptibility to SARS-CoV-2 infection is driven by the presence of ACE2 on host cells. Though ACE2 mRNA is present in nearly all organs, protein expression is predominantly localized to airway and alveolar epithelial cells, vascular endothelial cells, and alveolar macrophages [116]. Unlike SARS-CoV, SARS-COV-2's increased affinity for ACE2 allows it to establish infection in the nasal and oral tissues of the upper respiratory tract, including nasopharyngeal and oropharyngeal tissues[98]. Outside of the respiratory tract, ACE2 is also expressed on enterocytes in the small intestine[116]. As a result, SARS-CoV-2 is thought to be capable of establishing infection in both the upper and lower respiratory tract as well as the gastrointestinal tract[98].

COVID-19 Disease Presentation

SARS-CoV-2's tropism for cells of the respiratory and gastrointestinal tracts is evident in its disease presentation. The clinical implications of SARS-CoV-2 infection range from asymptomatic to severe influenza-like illness that may progress to respiratory failure and death[71,98]. According to the CDC, the most common symptoms associated with COVID-19 are fever or chills, cough, shortness of breath, difficulty breathing, fatigue, muscle or body aches, headache, loss of taste or smell, sore throat, congestion or runny nose, nausea or vomiting, and diarrhea[117]. In addition, risk factors for severe disease include age, preexisting conditions (including liver disease, obesity and dementia), African-American and Asian race, and male sex [118–120].

Transmission of SARS-CoV-2

SARS-CoV-2's tissue tropism and disease presentation directly correlate to its mode of transmission. Virus replication in the upper and lower respiratory tracts in addition to frequent coughing enables SARS-CoV-2 to be spread through respiratory droplets, contact (direct and close), fomites (indirect contact), and aerosols (airborne transmission) (Figure 1)[92,98]. As indicated by the width of the arrows in Figure 1, respiratory droplets are thought to be the predominant mode of transmission used by SARS-CoV-2[98]. Virus laced respiratory droplets, saliva, and other respiratory secretions are disseminated by symptomatic and asymptomatic individuals during normal speech, singing, sneezing, or coughing[98,121–124]. When susceptible individuals come into close or direct contact with an infected individual, these infectious secretions may interact with their mouth, nose, or eyes resulting in transmission[124]. Alternatively, these secretions or droplets can settle out of the air, contaminating objects and surfaces resulting in the generation of fomites[98,124]. These fomites are then able to contribute to transmission via indirect contact when naïve hosts interact with them then touch their eyes, nose, or mouth[98,124]. Airborne transmission via aerosols has also been reported during small, droplet nuclei generating medical procedures and may contribute to transmission in ventilation-poor indoor settings[124]. SARS-CoV-2's ability to infect cells of the gastrointestinal tract also suggests that fecal-oral transmission may be a plausible transmission route. Though no instances of fecal-oral transmission have been reported, three studies have been able to culture virus from stool samples[124–127].

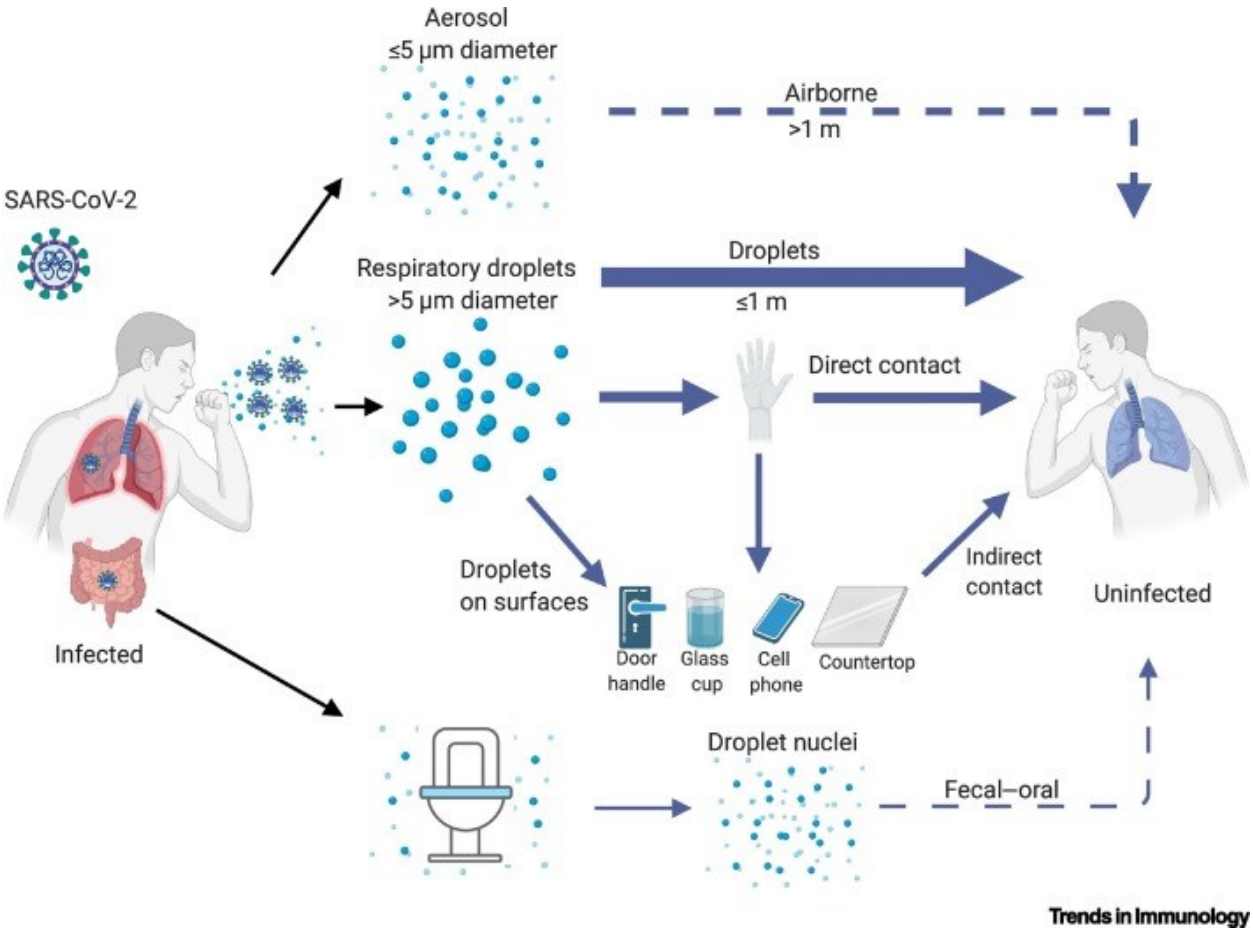

Figure 1. Proposed modes of transmission for SARS-CoV-2. Image from Harrison et al. (2020)[98] depicting proposed transmission routes for SARS-CoV-2. Solid arrow width indicates the relative contribution of each transmission route to viral spread. Dashed lines denote plausible transmission routes that had yet to be confirmed at the time of publication (December 2020).

Mutations in SARS-CoV02

Relative to DNA viruses, RNA viruses possess vastly higher rates of mutation. This is because the virus-encoded RNA dependent RNA polymerases responsible for replicating RNA virus genomes lack exonuclease proofreading ability [128]. As a result, whereas DNA viruses have between 10^{-8} to 10^{-6} substitutions per nucleotide site per cell infection (s/n/c), RNA viruses have 10^{-6} to 10^{-4} s/n/c [129]. What makes coronaviruses unique among the RNA viruses is that one of their proteins, nsp14, possesses a 3'-5' exonuclease (ExoN) [130]. By combining their functions, ExoN is able to remove mutagenic nucleotides erroneously inserted by the low fidelity RNA

polymerase resulting in faithful replication of the coronavirus genome and a lower mutation rate[97,130].

Though SARS-CoV-2's rate of mutation is decreased relative to other RNA viruses, the sheer number of hosts the virus is passing through combined with the number of replications it is undergoing in each individual vastly increases the likelihood of mutations occurring in the viral population [70]. In addition, as more individuals become infected and recover or become vaccinated, selective pressure favoring viral variants that escape naturally or vaccine induced immunity increases dramatically [131,132]. Therefore, as the pandemic progresses there is increasing concern that mutations will occur in epitopes recognized by the neutralizing antibodies responsible for conferring protection against SARS-CoV-2.

D614G Variant

One mutant that validated concerns of SARS-CoV-2 adaptation to human hosts is the Spike protein D614G variant. First identified by Korber et al.[70], D614G emerged in Europe and accounted for 10% of global sequences prior to March 1st. By May 18th, it represented 78% of sequences and had become the dominant strain infecting individuals in Europe, North America, Oceania, and Asia[70]. As the pandemic progresses, the D614G variant continues to represent an increasing proportion of sequences worldwide[133].

The D614G mutation occurs in the C-terminal region of the S1 domain of one protomer where it associates with the S2 domain of another protomer [134]. By replacing aspartic acid with glycine at residue 614, hydrogen bonding between protomers of the trimeric spike is disrupted, resulting in greater flexibility and altered interprotomer interactions[70]. Therefore, the protomers of the G614 S protein more easily transition from closed conformation, in which the RBD is

concealed, to the binding-competent open conformation, in which the RBD is oriented to interact with ACE2[133,135].

HYPOTHESIS

As the SARS-CoV-2 pandemic progresses, the likelihood of mutant viruses arising that evade preexisting immunity or become better suited to infecting humans is high[70]. One mutation that has swiftly arisen and become dominant in viral populations worldwide is D614G[70]. By replacing aspartic acid with glycine at this residue, interprotomer interactions within the trimeric spike of SARS-CoV-2 are disrupted, potentially allowing Spike proteins with G614 to have increased availability for binding to ACE2[133]. In this study, we sought to characterize differences in viral fitness induced by the D614G mutation by comparing the replication kinetics of D614 and G614 viruses in a primary human nasal epithelial cell culture system. We hypothesized that G614 viruses would replicate to significantly higher titers than D614 viruses on hNEC cultures, particularly at 37˚C, explaining why this variant has become prevalent in the viral population.

MATERIALS AND METHODS

Cell Lines

Vero E6/Transmembrane serine protease 2 (TMPRSS2) cells were cultured in DMEM supplemented with 10% FBS, 100U/mL penicillin with 100µg/mL streptomycin, and 1mM sodium pyruvate (Sigma-Aldrich) at 37˚C with 5% CO_2.

Human nasal epithelial cell (hNEC) cultures were isolated from the disease-free nasal tissue collected during endoscopic sinus surgery mandated for disease-unrelated conditions. The cells were then differentiated at the air-liquid interface (ALI) in 24-well Falcon filter inserts (0.4-µM pore; 0.33 cm^2; Becton Dickinson) at 37˚C with 5% CO_2. ALI medium containing 1X ALI maintenance supplement (STEMCELL Technologies), 0.192 µg/mL hydrocortisone stock solution (STEMCELL Technologies), and 5 IU/mL 0.2% heparin solution (STEMCELL Technologies) was used as basolateral medium.

Virus - Seed Stock and Working Stock

SARS-CoV-2 (isolate SARS-CoV-2/USA-Washington 1/2020) was provided by the CDC through BEI Resources. SARS-CoV-2/USA/MDHP-31/2020 (HP-31), SARS-CoV-2/USA/MDHP-76/2020 (HP-76), SARS-CoV-2/USA/DCHP-7/2020 (HP-7) and SARS-CoV-2/USA/MDHP-20/2020 (HP-20) were isolated from nasal swabs collected at Johns Hopkins Hospital. To produce seed stocks, virus was diluted to an MOI of 0.01 TCID50 units/cell in IM. Approximately 75% confluent T-150 (150 cm^2) flasks of TMPRSS2 cells were then washed twice with PBS + and infected with 5mL/flask of inoculum, rocking every 10 minutes for 1 hour at 32˚C with 5% CO_2. Each flask was then given 20mL of IM, incubated at 32˚C, and the progression of CPE monitored daily. Virus containing supernatant was collected when 70-90% CPE was achieved, approximately 4 days post infection. Infectious viral titer of the seed stocks

was then determined using TCID50 assays. Working stocks were produced in the same fashion using the steed stock to generate the viral inoculum.

TCID50 Assay

SARS-CoV-2 $TCID_{50}$ assays were conducted using 96-well plates of 75% confluent TMPRSS2 cells. After the cells were washed twice with PBS+, ten-fold serial dilutions of each virus in IM were produced, and 20µL applied to 6 wells of cells. The plates were then incubated at 37˚C with 5% CO_2 for 5 days. The cells were then fixed with 4% formaldehyde in PBS overnight and stained with Napthol Blue Black overnight. The resulting CPE was scored visually and the $TCID_{50}$ value for each sample was calculated using the Reed-Muench calculation [63].

Low MOI hNEC GC

Fully differentiated hNEC cells cultured on transwells in 24-well plates had their basolateral media collected and their apical surfaces washed three times by repeating the process of adding 100µL of IM with no NAT (IM-NAT), incubating for 10 minutes at 32˚C or 37˚C with 5% CO_2, then aspirating. The cells were then infected by adding 100µL of SARS-CoV-2 diluted to a MOI of 0.1 in IM-NAT to the apical surface for 2 hours at 32˚C or 37˚C with 5% CO_2. Following infection, the cells were washed three times with PBS- and then incubated at 32˚C or 37˚C with 5% CO_2. Apical samples were taken at 1, 12, 24, 36, 48, 72, 96, 120, 144, and 168 hours post infection by applying 100µL of IM-NAT to the apical surface, incubating at 32˚C or 37˚C for 10 minutes, and collecting. Basolateral supernatants were collected and replaced every 48 hours. Infectious viral titer was then quantified using $TCID_{50}$ assays.

Statistical Analysis

Low MOI GCs were analyzed by mixed ANOVA with repeated measures followed by a Tukey's multiple comparisons test. All statistical analyses were performed in GraphPad Prism 8.

RESULTS

Impact of the D614G mutation on SARS-CoV-2 replication in the upper versus lower respiratory tract

Viruses SARS-CoV-2/USA/MDHP-31/2020 (HP-31) and SARS-CoV-2/USA/MDHP-76/2020 (HP-76) have aspartic acid at position 614 (D614) and represent the viral population prior to the mutation event. SARS-CoV-2/USA/DCHP-7/2020 (HP-7) and SARS-CoV-2/USA/MDHP-20/2020 (HP-20) are variant viruses that possess a glycine at position 614 (G614). In order to compare the ability of pre- and post-mutation viruses to replicate in conditions consistent with the human upper versus lower respiratory tract, low MOI growth curves were conducted on hNEC cultures at either 32˚C or 37˚C.

Growth curves conducted at 32˚C were unsuccessful for all four viruses. Of the three growth curves conducted, the first (32 GC#1) has been evaluated in full (Figure 2A). HP-20 was the only virus found to be capable of infecting the hNECs and only half of the wells inoculated with the virus showed signs of viral replication. The remaining wells for all four viruses did not generate titers detectable by TCID50 assay. In order to avoid wasting resources on more failed experiments, only the inoculum and 48 hpi timepoints of the remaining two growth curves (32 GC#2 and #3) were titered (Figure 2B). Compared to 32 GC#1, more wells became infected in 32 GCs #2 and #3. However, HP-7 continued to have challenges infecting the hNEC cultures, as indicated by its position at or near the LOD. Additionally, titers for all four viruses at 48 hpi were lower than anticipated; at this point in infection, the virus is expected to be undergoing exponential replication, therefore the titer should be well above the initial, low MOI inoculum.

Growth curves conducted at 37˚C (37 GCs #1 and #2) were successful. In 37 GC#1 (Figure 3A), all four viruses showed exponential growth, reaching peak titer at 48 hpi. Though the viruses replicated similarly up until 48 hpi, D614 viral titers decreased at a significantly faster

rate than the G614 viruses. Though only inoculum and 48 hpi timepoints were titered for the second growth curve conducted at 37˚C (37 GC#2), exponential growth was observed for all four viruses and all wells became infected with virus (Figure 3B). Overall, these findings indicate that all four viruses were capable of effectively infecting hNEC cultures at 37˚C and suggest that G614 viruses maintain significantly higher levels of replication over time than D614 viruses.

(A)

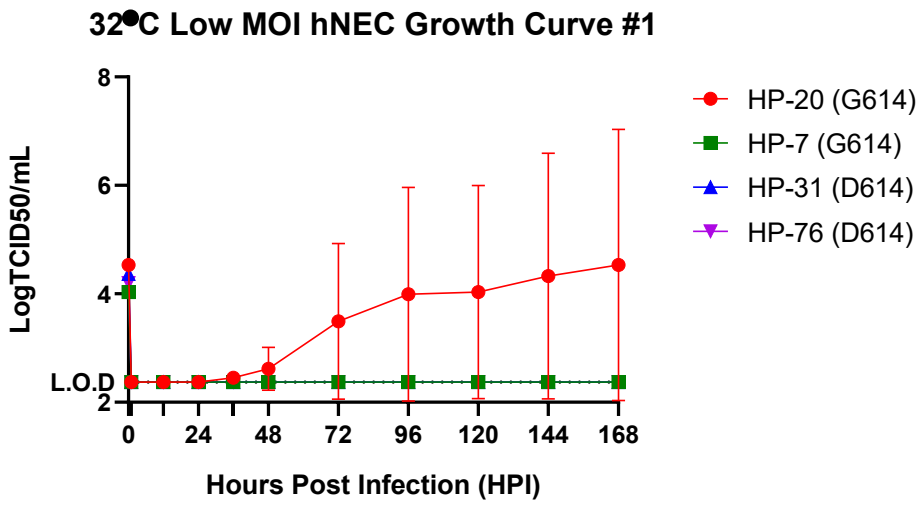

(B)

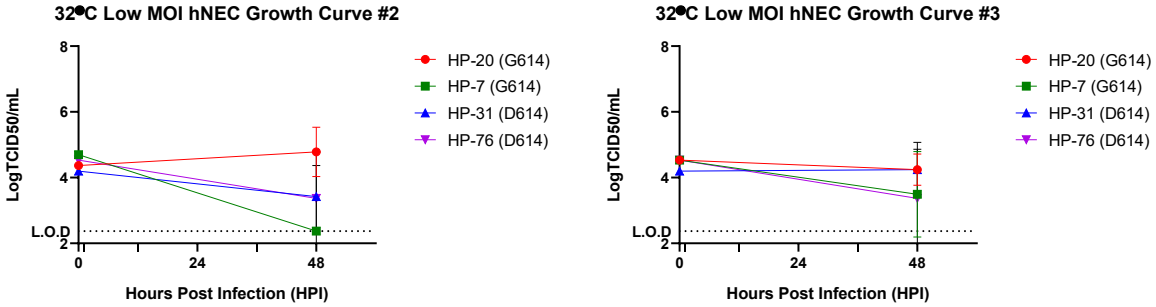

Figure 2. 32˚C growth curves comparing D614 and G614 viral replication on hNECs. Multi-step growth curves performed on differentiated hNEC cultures infected with an MOI of 0.1 at 32˚C. (A) Fully titered GC #1 demonstrating limited infection of hNEC cultures. (B) Inoculum and 48 hpi titers for GCs #2 and 3 illustrating improved but substandard infection of hNECs and minimal replication. L.O.D = 2.37 log TCID50/mL.

(A)

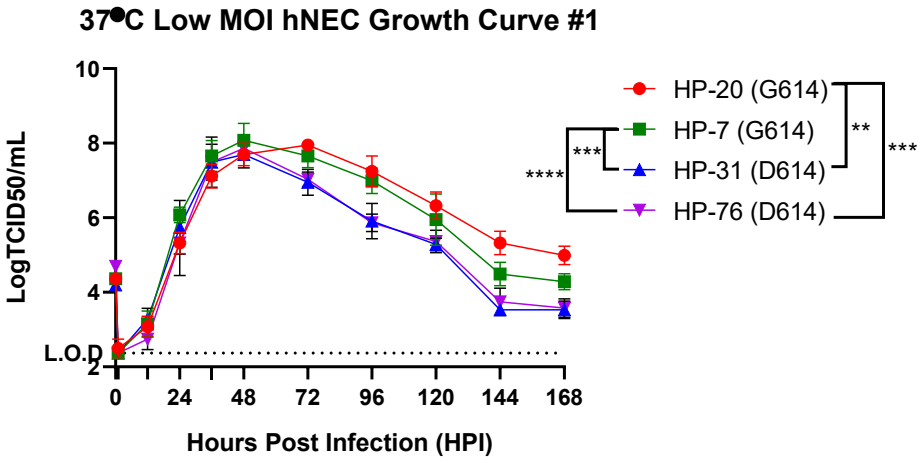

(B)

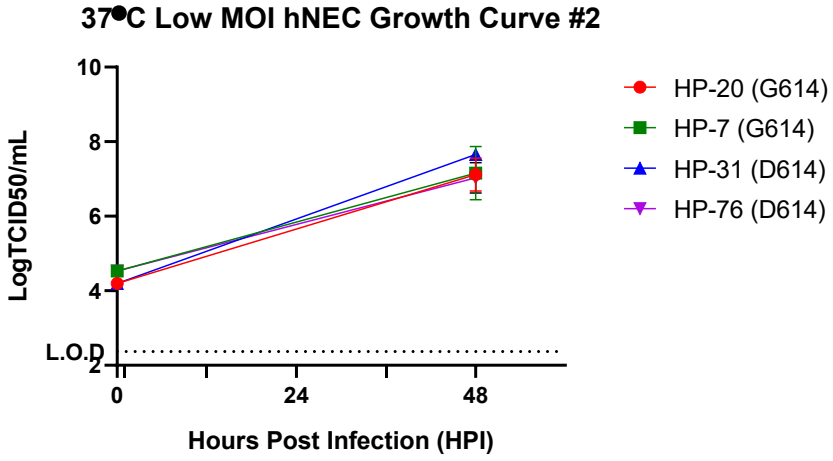

Figure 3. 37˚C growth curves comparing D614 and G614 viral replication on hNECs. (A) Multi-step growth curve performed on differentiated hNEC cultures infected with an MOI of 0.1 at 37˚C (37 GC#1). Statistical significance was measured using a MANOVA with repeated measures followed by a Tukey's post-test. Results are from one experiment with four biological replicates. **p<0.01, ***p<0.001, ****p<0.0001. L.O.D = 2.37 log TCID50/mL. (B) Inoculum and 48 hpi titers for 37 GC #2, illustrating consistent infection of hNECs and high viral titers for all four viruses at 48 hpi.

DISCUSSION

Impact of the D614G mutation on SARS-CoV-2 replication kinetics in hNECs at 32˚C and 37˚C

In early April 2020, SARS-CoV-2 viruses containing a mutation in the spike protein, D614G, became the dominant virus lineage, suggesting the mutation conferred an advantage over the original virus[70]. To understand the implications of the D614G mutation on SARS-CoV-2 replication at temperatures representative of the upper (32˚C) and lower (37˚C) respiratory tract, low MOI hNEC growth curves comparing D614 and G614 viruses were carried out. Our preliminary data suggests that all four viruses productively infect hNEC cultures at 37˚C but fail to replicate efficiently at 32˚C. Further quantification of viral titers over the course of infection are needed to fully elucidate the effect of the D614G mutation on viral replication.

Several articles investigating the implications of the D614G mutation have been published over the course of the pandemic. In the seminal paper raising concerns about this variant, the authors attributed the prolific spread of G614 viruses to higher infectivity as indicated by replication to higher viral titers and higher patient Ct values suggesting higher *in vivo* viral loads[70]. The mechanism by which G614 viruses are able to generate higher viral loads is currently being investigated. In a paper by Daniloski et al.[136], SARS-CoV-2-psueudotyped lentiviral particles produced using site-directed mutagenesis demonstrated G614 viruses were significantly more effective at entering human cells. Though ACE2 receptor binding was almost identical between the viruses, the G614 spike was found to be resistant to proteolytic cleavage during protein production, suggesting that these viruses are more infectious due to the presence of more functional (uncleaved) S protein per virion[134,136]. Other articles agree that D614G confers enhanced cellular entry, but indicate that higher affinity for ACE2, rather than protection from cleavage, is responsible for the advantage[133,137]. Overall, the greater infection efficiency

conveyed by D614G is currently considered a leading hypothesis explaining the domination of G614 variants in viral populations world wide[138–140].

The clinical implications of the D614G mutation are thought to be limited. Several studies have shown patients infected with G614 versus D614 viruses do not show evidence of increased disease severity[70,141]. Additionally, convalescent plasma generated in response to D614 infection has been shown to be cross protective against G614 infection, suggesting current vaccines generated against the original D614 virus will be effective against G614 variants[133,139,142].

FUTURE DIRECTIONS

Impact of the D614G mutation on SARS-CoV-2 replication kinetics in hNECs at 37˚C

The preliminary data generated by this study demonstrated that both D614 and G614 viruses are susceptible to variations in temperature, lacking efficient replication at 32˚C. However, the goal of this study was to determine whether the D614G mutation altered viral fitness in conditions consistent with the upper and lower respiratory tract. In order to accomplish this, the conditions of the 32˚C growth curves must be altered to maximize viral infectivity and the remaining 37˚C growth curves must be titered. Therefore, it is necessary to identify alterations in the low MOI GC protocol that may allow for the success of the 32˚C GCs. TMPRSS2 growth curves further exploring in the impact of 32˚C and testing alterations in MOI need to be conducted to optimize these conditions and then apply them to hNECs. Since our virus working stocks are generated by infection VeroTMPRSS2 cells at 32˚C with a low MOI, I hypothesize that the inability to efficiently infect hNECs at that temperature has to do with the infection of epithelial cells rather than a strict inability to infect because of temperature.

Additionally, we preliminarily showed that all four viruses tested were capable of efficient replication on fully differentiated hNEC cultures at 37˚C, with G614 viruses maintaining significantly higher titers for more prolonged periods of time in comparison to D614 viruses. In order to confidently discern differences between D614 and G614 viruses at this temperature, GCs #2 and #3 must be titered. By optimizing the 32˚C GCs and comparing them to fully titered 37˚C GCs we will be able to observe the effect of the D614G mutation on viral replication kinetics in a cell culture system representative of the human upper respiratory tract.

Also, in this study we are relying on TCID50 assays which only provide information on the amount of infectious virus. Further studies comparing genome copies to plaque forming units (PFU) may be necessary to determine whether the D614G mutation is impacting viral replication

resulting the generation of more viral particles [more genomes and more PFUs] or whether it impacts the amount of infectious viral particles generated [same amount of genomes but more PFUs].

REFERENCES

1. Collin EA, Sheng Z, Lang Y, Ma W, Hause BM, Li F. Cocirculation of Two Distinct Genetic and Antigenic Lineages of Proposed Influenza D Virus in Cattle. *J Virol*. 2014;89(2):1036-1042. doi:10.1128/JVI.02718-14

2. Samji T. Influenza A: Understanding the Viral Life Cycle. *Yale J Biol Med*. 2009;82(4):153-159.

3. Taubenberger JK, Kash JC. Influenza Virus Evolution, Host Adaptation and Pandemic Formation. *Cell Host Microbe*. 2010;7(6):440-451. doi:10.1016/j.chom.2010.05.009

4. Wang M, Veit M. Hemagglutinin-esterase-fusion (HEF) protein of influenza C virus. *Protein Cell*. 2016;7(1):28-45. doi:10.1007/s13238-015-0193-x

5. Hause BM, Collin EA, Liu R, et al. Characterization of a Novel Influenza Virus in Cattle and Swine: Proposal for a New Genus in the Orthomyxoviridae Family. *mBio*. 2014;5(2). doi:10.1128/mBio.00031-14

6. Su S, Fu X, Li G, Kerlin F, Veit M. Novel Influenza D virus: Epidemiology, pathology, evolution and biological characteristics. *Virulence*. 2017;8(8):1580-1591. doi:10.1080/21505594.2017.1365216

7. Hause BM, Ducatez M, Collin EA, et al. Isolation of a novel swine influenza virus from Oklahoma in 2011 which is distantly related to human influenza C viruses. *PLoS Pathog*. 2013;9(2):e1003176. doi:10.1371/journal.ppat.1003176

8. Song H, Qi J, Khedri Z, et al. An Open Receptor-Binding Cavity of Hemagglutinin-Esterase-Fusion Glycoprotein from Newly-Identified Influenza D Virus: Basis for Its Broad Cell Tropism. *PLoS Pathog*. 2016;12(1). doi:10.1371/journal.ppat.1005411

9. Liu R, Sreenivasan C, Yu H, et al. Influenza D virus diverges from its related influenza C virus in the recognition of 9-O-acetylated N-acetyl- or N-glycolyl-neuraminic acid-containing glycan receptors. *Virology*. 2020;545:16-23. doi:10.1016/j.virol.2020.02.007

10. Wasik BR, Barnard KN, Ossiboff RJ, et al. Distribution of O-Acetylated Sialic Acids among Target Host Tissues for Influenza Virus. *mSphere*. 2017;2(5). doi:10.1128/mSphere.00379-16

11. Foni E, Chiapponi C, Baioni L, et al. Influenza D in Italy: towards a better understanding of an emerging viral infection in swine. *Sci Rep*. 2017;7(1):11660. doi:10.1038/s41598-017-12012-3

12. Lee J, Wang L, Palinski R, et al. Comparison of Pathogenicity and Transmissibility of Influenza B and D Viruses in Pigs. *Viruses*. 2019;11(10). doi:10.3390/v11100905

13. Asha K, Kumar B. Emerging Influenza D Virus Threat: What We Know so Far! *J Clin Med*. 2019;8(2). doi:10.3390/jcm8020192

14. Falchi A. Influenza D Virus: The Most Discreet (for the Moment?) of the Influenza Viruses. *J Clin Med*. 2020;9(8). doi:10.3390/jcm9082550

15. Mills J, V, Chanock RM, Nusinoff SR, Walls BE, Fishburne IE. Temperature-Sensitive Mutants of Influenza Virus. I. Behavior in Tissue Culture and in Experimental Animals. *J Infect Dis*. 1971;123(2):145-157.

16. Bailey ES, Fieldhouse JK, Alarja NA, et al. First sequence of influenza D virus identified in poultry farm bioaerosols in Sarawak, Malaysia. *Trop Dis Travel Med Vaccines*. 2020;6(1):5. doi:10.1186/s40794-020-0105-9

17. Ferguson L, Olivier AK, Genova S, et al. Pathogenesis of Influenza D Virus in Cattle. *J Virol*. 2016;90(12):5636-5642. doi:10.1128/JVI.03122-15

18. Salem E, Hägglund S, Cassard H, et al. Pathogenesis, Host Innate Immune Response, and Aerosol Transmission of Influenza D Virus in Cattle. *J Virol*. 2019;93(7). doi:10.1128/JVI.01853-18

19. Kaplan BS, Falkenberg S, Dassanayake R, et al. Virus Strain Influenced the Interspecies Transmission of Influenza D Virus Between Calves and Pigs. *Transbound Emerg Dis*. Published online December 1, 2020. doi:https://doi.org/10.1111/tbed.13943

20. Hause BM, Huntimer L, Falkenberg S, Henningson J, Lechtenberg K, Halbur T. An inactivated influenza D virus vaccine partially protects cattle from respiratory disease caused by homologous challenge. *Vet Microbiol*. 2017;199:47-53. doi:10.1016/j.vetmic.2016.12.024

21. Sreenivasan C, Thomas M, Sheng Z, et al. Replication and Transmission of the Novel Bovine Influenza D Virus in a Guinea Pig Model. *J Virol*. 2015;89(23):11990-12001. doi:10.1128/JVI.01630-15

22. Mitra N, Cernicchiaro N, Torres S, Li F, Hause BM. Metagenomic characterization of the virome associated with bovine respiratory disease in feedlot cattle identified novel viruses and suggests an etiologic role for influenza D virus. *J Gen Virol*. 2016;97(8):1771-1784. doi:10.1099/jgv.0.000492

23. Beef Cattle Research Council. Bovine Respiratory Disease. Published October 2, 2019. Accessed February 27, 2021. http://www.beefresearch.ca/research-topic.cfm

24. Ng TFF, Kondov NO, Deng X, Van Eenennaam A, Neibergs HL, Delwart E. A Metagenomics and Case-Control Study To Identify Viruses Associated with Bovine Respiratory Disease. *J Virol*. 2015;89(10):5340-5349. doi:10.1128/JVI.00064-15

25. Ferguson L, Eckard L, Epperson WB, et al. Influenza D virus infection in Mississippi beef cattle. *Virology*. 2015;486:28-34. doi:10.1016/j.virol.2015.08.030

26. Belser JA, Katz JM, Tumpey TM. The ferret as a model organism to study influenza A virus infection. *Dis Model Mech*. 2011;4(5):575-579. doi:10.1242/dmm.007823

27. Maher JA, DeStefano J. The Ferret: An Animal Model to Study Influenza Virus. *Lab Anim*. 2004;33(9):50-53. doi:10.1038/laban1004-50

28. Belser JA, Barclay W, Barr I, et al. Ferrets as Models for Influenza Virus Transmission Studies and Pandemic Risk Assessments. *Emerg Infect Dis*. 2018;24. doi:10.3201/eid2406.172114

29. Gorin S, Fablet C, Quéguiner S, et al. Assessment of Influenza D Virus in Domestic Pigs and Wild Boars in France: Apparent Limited Spread within Swine Populations Despite Serological Evidence of Breeding Sow Exposure. *Viruses*. 2019;12(1). doi:10.3390/v12010025

30. O'Donovan T, Donohoe L, Ducatez MF, Meyer G, Ryan E. Seroprevalence of influenza D virus in selected sample groups of Irish cattle, sheep and pigs. *Ir Vet J*. 2019;72. doi:10.1186/s13620-019-0150-8

31. Zhai S-L, Zhang H, Chen S-N, et al. Influenza D Virus in Animal Species in Guangdong Province, Southern China. *Emerg Infect Dis*. 2017;23(8):1392-1396. doi:10.3201/eid2308.170059

32. Oliva J, Eichenbaum A, Belin J, et al. Serological Evidence of Influenza D Virus Circulation Among Cattle and Small Ruminants in France. *Viruses*. 2019;11(6). doi:10.3390/v11060516

33. Quast M, Sreenivasan C, Sexton G, et al. Serological evidence for the presence of influenza D virus in small ruminants. *Vet Microbiol*. 2015;180(0):281-285. doi:10.1016/j.vetmic.2015.09.005

34. Salem E, Cook EAJ, Lbacha HA, et al. Serologic Evidence for Influenza C and D Virus among Ruminants and Camelids, Africa, 1991–2015. *Emerg Infect Dis*. 2017;23(9):1556-1559. doi:10.3201/eid2309.170342

35. Murakami S, Odagiri T, Melaku SK, et al. Influenza D Virus Infection in Dromedary Camels, Ethiopia. *Emerg Infect Dis*. 2019;25(6):1224-1226. doi:10.3201/eid2506.181158

36. Nedland H, Wollman J, Sreenivasan C, et al. Serological evidence for the co-circulation of two lineages of influenza D viruses in equine populations of the Midwest United States. *Zoonoses Public Health*. 2018;65(1):e148-e154. doi:10.1111/zph.12423

37. Rosignoli C, Faccini S, Merenda M, et al. Influenza D virus infection in cattle in Italy. *Large Anim Rev*. 2017;23(4):123-128.

38. Chiapponi C, Faccini S, Fusaro A, et al. Detection of a New Genetic Cluster of Influenza D Virus in Italian Cattle. *Viruses*. 2019;11(12). doi:10.3390/v11121110

39. Chiapponi C, Faccini S, De Mattia A, et al. Detection of Influenza D Virus among Swine and Cattle, Italy. *Emerg Infect Dis*. 2016;22(2):352-354. doi:10.3201/eid2202.151439

40. Dane H, Duffy C, Guelbenzu M, et al. Detection of influenza D virus in bovine respiratory disease samples, UK. *Transbound Emerg Dis*. 2019;66(5):2184-2187. doi:10.1111/tbed.13273

41. Ducatez MF, Pelletier C, Meyer G. Influenza D Virus in Cattle, France, 2011–2014. *Emerg Infect Dis*. 2015;21(2):368-371. doi:10.3201/eid2102.141449

42. Flynn O, Gallagher C, Mooney J, et al. Influenza D Virus in Cattle, Ireland. *Emerg Infect Dis*. 2018;24(2):389-391. doi:10.3201/eid2402.170759

43. Jiang W-M, Wang S-C, Peng C, et al. Identification of a potential novel type of influenza virus in Bovine in China. *Virus Genes*. 2014;49(3):493-496. doi:10.1007/s11262-014-1107-3

44. Snoeck CJ, Oliva J, Pauly M, et al. Influenza D Virus Circulation in Cattle and Swine, Luxembourg, 2012–2016. *Emerg Infect Dis*. 2018;24(7):1388-1389. doi:10.3201/eid2407.171937

45. Yilmaz A, Umar S, Turan N, et al. First report of influenza D virus infection in Turkish cattle with respiratory disease. *Res Vet Sci*. 2020;130:98-102. doi:10.1016/j.rvsc.2020.02.017

46. Murakami S, Endoh M, Kobayashi T, et al. Influenza D Virus Infection in Herd of Cattle, Japan. *Emerg Infect Dis*. 2016;22(8):1517-1519. doi:http://dx.doi.org/10.3201/eid2208.160362

47. Murakami S, Sato R, Ishida H, Katayama M, Takenaka-Uema A, Horimoto T. Influenza D Virus of New Phylogenetic Lineage, Japan. *Emerg Infect Dis*. 2020;26(1):168-171. doi:10.3201/eid2601.191092

48. Alvarez IJ, Fort M, Pasucci J, et al. Seroprevalence of influenza D virus in bulls in Argentina. *J Vet Diagn Investig Off Publ Am Assoc Vet Lab Diagn Inc*. 2020;32(4):585-588. doi:10.1177/1040638720934056

49. Skelton R. Influenza D Virus, Secondary Bacterial Infections, and the Immune Response—Oh My! *IdeaFest*. Published online May 1, 2020. https://red.library.usd.edu/idea/69

50. Hause BM, Collin EA, Anderson J, Hesse RA, Anderson G. Bovine Rhinitis Viruses Are Common in U.S. Cattle with Bovine Respiratory Disease. *PLOS ONE*. 2015;10(3):e0121998. doi:10.1371/journal.pone.0121998

51. Luo J, Ferguson L, Smith DR, Woolums AR, Epperson WB, Wan X-F. Serological evidence for high prevalence of Influenza D Viruses in Cattle, Nebraska, United States, 2003-2004. *Virology*. 2017;501:88-91. doi:10.1016/j.virol.2016.11.004

52. Sreenivasan CC, Thomas M, Kaushik RS, Wang D, Li F. Influenza A in Bovine Species: A Narrative Literature Review. *Viruses*. 2019;11(6):561. doi:10.3390/v11060561

53. Liu R, Sheng Z, Huang C, Wang D, Li F. Influenza D virus. *Curr Opin Virol*. 2020;44:154-161. doi:10.1016/j.coviro.2020.08.004

54. Parrish CR, Murcia PR, Holmes EC. Influenza Virus Reservoirs and Intermediate Hosts: Dogs, Horses, and New Possibilities for Influenza Virus Exposure of Humans. Schultz-Cherry S, ed. *J Virol*. 2015;89(6):2990-2994. doi:10.1128/JVI.03146-14

55. CDC. Transmission of Avian Influenza A Viruses Between Animals and People | Avian Influenza (Flu). Published February 10, 2015. Accessed February 2, 2021. https://www.cdc.gov/flu/avianflu/virus-transmission.htm

56. CDC. CDC H1N1 Flu | Origin of 2009 H1N1 Flu (Swine Flu). Published November 25, 2009. Accessed February 2, 2021. https://www.cdc.gov/h1n1flu/information_h1n1_virus_qa.htm

57. Wan X-F, Ferguson L, Oliva J, et al. Limited cross-protection provided by prior infection contributes to high prevalence of influenza D viruses in cattle. *J Virol*. Published online July 1, 2020. doi:10.1128/JVI.00240-20

58. Smith DB, Gaunt ER, Digard P, Templeton K, Simmonds P. Detection of influenza C virus but not influenza D virus in Scottish respiratory samples. *J Clin Virol*. 2016;74:50-53. doi:10.1016/j.jcv.2015.11.036

59. White SK, Ma W, McDaniel CJ, Gray GC, Lednicky JA. Serologic evidence of exposure to influenza D virus among persons with occupational contact with cattle. *J Clin Virol*. 2016;81:31-33. doi:10.1016/j.jcv.2016.05.017

60. Trombetta CM, Marchi S, Manini I, et al. Influenza D Virus: Serological Evidence in the Italian Population from 2005 to 2017. *Viruses*. 2019;12(1). doi:10.3390/v12010030

61. Eckard L. Assessment of the Zoonotic Potential of a Novel Bovine Influenza Virus. *Theses Diss ETD*. Published online May 1, 2016. doi:10.21007/etd.cghs.2016.0405

62. Thielen P, Nolting JM, Nelson SW, Mehoke TS, Howser C, Bowman AS. Complete Genome Sequence of an Influenza D Virus Strain Identified in a Pig with Subclinical Infection in the United States. *Microbiol Resour Announc*. 2019;8(4). doi:10.1128/MRA.01462-18

63. Reed LJ, Muench H. A SIMPLE METHOD OF ESTIMATING FIFTY PER CENT ENDPOINTS. *Am J Hyg*. 1938;27(3):5.

64. Wohlgemuth N, Ye Y, Fenstermacher KJ, Liu H, Lane AP, Pekosz A. The M2 protein of live, attenuated influenza vaccine encodes a mutation that reduces replication in human nasal epithelial cells. *Vaccine*. 2017;35(48 Pt B):6691-6699. doi:10.1016/j.vaccine.2017.10.018

65. Forero A, Fenstermacher K, Wohlgemuth N, et al. Evaluation of the innate immune responses to influenza and live-attenuated influenza vaccine infection in primary

differentiated human nasal epithelial cells. *Vaccine*. 2017;35(45):6112-6121. doi:10.1016/j.vaccine.2017.09.058

66. Takada K, Kawakami C, Fan S, et al. A humanized MDCK cell line for the efficient isolation and propagation of human influenza viruses. *Nat Microbiol*. 2019;4(8):1268-1273. doi:10.1038/s41564-019-0433-6

67. Barnard KN, Wasik BR, LaClair JR, et al. Expression of 9-O- and 7,9-O-Acetyl Modified Sialic Acid in Cells and Their Effects on Influenza Viruses. 2019;10(6):17.

68. Holwerda M, Kelly J, Laloli L, et al. Determining the Replication Kinetics and Cellular Tropism of Influenza D Virus on Primary Well-Differentiated Human Airway Epithelial Cells. *Viruses*. 2019;11(4). doi:10.3390/v11040377

69. Klein SL, Pekosz A, Park H-S, et al. Sex, age, and hospitalization drive antibody responses in a COVID-19 convalescent plasma donor population. doi:10.1172/JCI142004

70. Korber B, Fischer WM, Gnanakaran S, et al. Tracking Changes in SARS-CoV-2 Spike: Evidence that D614G Increases Infectivity of the COVID-19 Virus. *Cell*. 2020;182(4):812-827.e19. doi:10.1016/j.cell.2020.06.043

71. Zhou P, Yang X-L, Wang X-G, et al. A pneumonia outbreak associated with a new coronavirus of probable bat origin. *Nature*. 2020;579(7798):270-273. doi:10.1038/s41586-020-2012-7

72. Klasse PJ. Neutralization of Virus Infectivity by Antibodies: Old Problems in New Perspectives. Advances in Biology. doi:https://doi.org/10.1155/2014/157895

73. VanBlargan LA, Goo L, Pierson TC. Deconstructing the Antiviral Neutralizing-Antibody Response: Implications for Vaccine Development and Immunity. *Microbiol Mol Biol Rev*. 2016;80(4):989-1010. doi:10.1128/MMBR.00024-15

74. Benner SE, Patel EU, Laeyendecker O, et al. SARS-CoV-2 Antibody Avidity Responses in COVID-19 Patients and Convalescent Plasma Donors. *J Infect Dis*. 2020;222(12):1974-1984. doi:10.1093/infdis/jiaa581

75. Bloch EM, Patel EU, Marshall C, et al. ABO blood group and SARS-CoV-2 antibody response in a convalescent donor population. *Vox Sang*. Published online January 25, 2021. doi:10.1111/vox.13070

76. Heaney CD, Pisanic N, Randad PR, et al. Comparative performance of multiplex salivary and commercially available serologic assays to detect SARS-CoV-2 IgG and neutralization titers. *medRxiv*. Published online February 1, 2021:2021.01.28.21250717. doi:10.1101/2021.01.28.21250717

77. Kared H, Redd AD, Bloch EM, et al. SARS-CoV-2–specific $CD8^+$ T cell responses in convalescent COVID-19 individuals. *J Clin Invest*. 2021;131(5). doi:10.1172/JCI145476

78. Long Q-X, Tang X-J, Shi Q-L, et al. Clinical and immunological assessment of asymptomatic SARS-CoV-2 infections. *Nat Med*. 2020;26(8):1200-1204. doi:10.1038/s41591-020-0965-6

79. Hinton DM. Letter of Authorization, Reissuance of Convalescent Plasma EUA November 30, 2020. Published online November 30, 2020. https://www.fda.gov/media/141477/download

80. Morgenlander WR, Henson SN, Monaco DR, et al. Antibody responses to endemic coronaviruses modulate COVID-19 convalescent plasma functionality. *J Clin Invest*. Published online February 11, 2021. doi:10.1172/JCI146927

81. Morgenlander W, Henson S, Monaco D, et al. Antibody responses to endemic coronaviruses modulate COVID-19 convalescent plasma functionality. *medRxiv*. Published online December 18, 2020:2020.12.16.20248294. doi:10.1101/2020.12.16.20248294

82. Ogega CO, Skinner NE, Blair PW, et al. Durable SARS-CoV-2 B cell immunity after mild or severe disease. *J Clin Invest*. Published online February 11, 2021. doi:10.1172/JCI145516

83. Patel EU, Bloch EM, Clarke W, et al. Comparative Performance of Five Commercially Available Serologic Assays To Detect Antibodies to SARS-CoV-2 and Identify Individuals with High Neutralizing Titers. *J Clin Microbiol*. 2021;59(2). doi:10.1128/JCM.02257-20

84. Li Q, Guan X, Wu P, et al. Early Transmission Dynamics in Wuhan, China, of Novel Coronavirus–Infected Pneumonia. *N Engl J Med*. 2020;382(13):1199-1207. doi:10.1056/NEJMoa2001316

85. Zhu N, Zhang D, Wang W, et al. A Novel Coronavirus from Patients with Pneumonia in China, 2019. *N Engl J Med*. 2020;382(8):727-733. doi:10.1056/NEJMoa2001017

86. Brüssow H. The Novel Coronavirus – A Snapshot of Current Knowledge. *Microb Biotechnol*. 2020;13(3):607-612. doi:10.1111/1751-7915.13557

87. World Health Organization. Novel Coronavirus (2019-nCoV): Situation Report -1. Published online January 21, 2020. https://www.who.int/docs/default-source/coronaviruse/situation-reports/20200121-sitrep-1-2019-ncov.pdf?sfvrsn=20a99c10_4

88. Guan W, Ni Z, Hu Y, et al. Clinical Characteristics of Coronavirus Disease 2019 in China. *N Engl J Med*. Published online February 28, 2020. doi:10.1056/NEJMoa2002032

89. Wang H, Li X, Li T, et al. The genetic sequence, origin, and diagnosis of SARS-CoV-2. *Eur J Clin Microbiol Infect Dis*. Published online April 24, 2020:1-7. doi:10.1007/s10096-020-03899-4

90. Wu F, Zhao S, Yu B, et al. A new coronavirus associated with human respiratory disease in China. *Nature*. 2020;579(7798):265-269. doi:10.1038/s41586-020-2008-3

91. World Health Organization. COVID-19 Weekly Epidemiological Update - 29 December 2020. Published online December 27, 2020. https://www.who.int/publications/m/item/weekly-epidemiological-update---29-december-2020

92. Cucinotta D, Vanelli M. WHO Declares COVID-19 a Pandemic. *Acta Bio Medica Atenei Parm*. 2020;91(1):157-160. doi:10.23750/abm.v91i1.9397

93. WHO Coronavirus (COVID-19) Dashboard. Accessed April 2, 2021. https://covid19.who.int

94. Payne S. Family Coronaviridae. *Viruses*. Published online 2017:149-158. doi:10.1016/B978-0-12-803109-4.00017-9

95. Tang Q, Song Y, Shi M, Cheng Y, Zhang W, Xia X-Q. Inferring the hosts of coronavirus using dual statistical models based on nucleotide composition. *Sci Rep*. 2015;5(1):17155. doi:10.1038/srep17155

96. Chen Y, Liu Q, Guo D. Emerging coronaviruses: Genome structure, replication, and pathogenesis. *J Med Virol*. 2020;92(4):418-423. doi:10.1002/jmv.25681

97. Fani M, Teimoori A, Ghafari S. Comparison of the COVID-2019 (SARS-CoV-2) pathogenesis with SARS-CoV and MERS-CoV infections. *Future Virol*. Published online May 20, 2020. doi:10.2217/fvl-2020-0050

98. Harrison AG, Lin T, Wang P. Mechanisms of SARS-CoV-2 Transmission and Pathogenesis. *Trends Immunol*. 2020;41(12):1100-1115.

99. Perlman S, Netland J. Coronaviruses post-SARS: update on replication and pathogenesis. *Nat Rev Microbiol*. 2009;7(6):439-450. doi:10.1038/nrmicro2147

100. Örd M, Faustova I, Loog M. The sequence at Spike S1/S2 site enables cleavage by furin and phospho-regulation in SARS-CoV2 but not in SARS-CoV1 or MERS-CoV. *Sci Rep*. 2020;10(1):16944. doi:10.1038/s41598-020-74101-0

101. Mendonça L, Howe A, Gilchrist JB, et al. SARS-CoV-2 Assembly and Egress Pathway Revealed by Correlative Multi-modal Multi-scale Cryo-imaging. *bioRxiv*. Published online November 5, 2020:2020.11.05.370239. doi:10.1101/2020.11.05.370239

102. World Health Organization. Summary of probable SARS cases with onset of illness from 1 November 2002 to 31 July 2003. Published July 24, 2015. Accessed January 17, 2021. https://www.who.int/publications/m/item/summary-of-probable-sars-cases-with-onset-of-illness-from-1-november-2002-to-31-july-2003

103. Ren W, Li W, Yu M, et al. Full-length genome sequences of two SARS-like coronaviruses in horseshoe bats and genetic variation analysis. *J Gen Virol*. 2006;87(11):3355-3359. doi:10.1099/vir.0.82220-0

104. Guan Y, Zheng BJ, He YQ, et al. Isolation and Characterization of Viruses Related to the SARS Coronavirus from Animals in Southern China. *Science*. 2003;302(5643):276-278. doi:10.1126/science.1087139

105. World Health Organization. WHO MERS Global Summary and Assessment of Risk. Published online August 2018. https://www.who.int/csr/disease/coronavirus_infections/risk-assessment-august-2018.pdf?ua=1

106. Sikkema RS, Farag E a. BA, Islam M, et al. Global status of Middle East respiratory syndrome coronavirus in dromedary camels: a systematic review. *Epidemiol Infect*. 2019;147. doi:10.1017/S095026881800345X

107. Lu R, Zhao X, Li J, et al. Genomic characterisation and epidemiology of 2019 novel coronavirus: implications for virus origins and receptor binding. *The Lancet*. 2020;395(10224):565-574. doi:10.1016/S0140-6736(20)30251-8

108. Tan W, Zhao X, Ma X, et al. A Novel Coronavirus Genome Identified in a Cluster of Pneumonia Cases - Wuhan, China 2019-2020. *China CDC Wkly*. 2020;2(4):57-60. doi:10.46234/ccdcw2020.016

109. Zheng J. SARS-CoV-2: an Emerging Coronavirus that Causes a Global Threat. *Int J Biol Sci*. 2020;16(10):1678-1685. doi:10.7150/ijbs.45053

110. Vilcek S. SARS-CoV-2: Zoonotic origin of pandemic coronavirus. *Acta Virol*. 2020;64(3):281-287. doi:10.4149/av_2020_302

111. Zhang T, Wu Q, Zhang Z. Probable Pangolin Origin of SARS-CoV-2 Associated with the COVID-19 Outbreak. *Curr Biol*. 2020;30(7):1346-1351.e2. doi:10.1016/j.cub.2020.03.022

112. Xiao K, Zhai J, Feng Y, et al. Isolation of SARS-CoV-2-related coronavirus from Malayan pangolins. *Nature*. 2020;583(7815):286-289. doi:10.1038/s41586-020-2313-x

113. Wrapp D, Wang N, Corbett KS, et al. Cryo-EM structure of the 2019-nCoV spike in the prefusion conformation. *Science*. 2020;367(6483):1260-1263. doi:10.1126/science.abb2507

114. Shang J, Wan Y, Luo C, et al. Cell entry mechanisms of SARS-CoV-2. *Proc Natl Acad Sci U S A*. 2020;117(21):11727-11734. doi:10.1073/pnas.2003138117

115. Hoffmann M, Kleine-Weber H, Schroeder S, et al. SARS-CoV-2 Cell Entry Depends on ACE2 and TMPRSS2 and Is Blocked by a Clinically Proven Protease Inhibitor. *Cell*. Published online March 2020:S0092867420302294. doi:10.1016/j.cell.2020.02.052

116. Hamming I, Timens W, Bulthuis M, Lely A, Navis G, van Goor H. Tissue distribution of ACE2 protein, the functional receptor for SARS coronavirus. A first step in understanding SARS pathogenesis. *J Pathol*. 2004;203(2):631-637. doi:10.1002/path.1570

117. CDC. Coronavirus Disease 2019 (COVID-19) – Symptoms. Centers for Disease Control and Prevention. Published December 22, 2020. Accessed January 21, 2021. https://www.cdc.gov/coronavirus/2019-ncov/symptoms-testing/symptoms.html

118. Li G, Liu Y, Jing X, et al. Mortality risk of COVID-19 in elderly males with comorbidities: a multi-country study. *Aging*. 2020;13(1):27-60. doi:10.18632/aging.202456

119. CDC. COVID-19 and Your Health. Centers for Disease Control and Prevention. Published February 11, 2020. Accessed January 21, 2021. https://www.cdc.gov/coronavirus/2019-ncov/need-extra-precautions/index.html

120. Bennett TD, Moffitt RA, Hajagos JG, et al. The National COVID Cohort Collaborative: Clinical Characterization and Early Severity Prediction. *MedRxiv Prepr Serv Health Sci*. Published online January 13, 2021. doi:10.1101/2021.01.12.21249511

121. Tang S, Mao Y, Jones RM, et al. Aerosol transmission of SARS-CoV-2? Evidence, prevention and control. *Environ Int*. 2020;144:106039. doi:10.1016/j.envint.2020.106039

122. Dhand R, Li J. Coughs and Sneezes: Their Role in Transmission of Respiratory Viral Infections, Including SARS-CoV-2. *Am J Respir Crit Care Med*. 2020;202(5):651-659. doi:10.1164/rccm.202004-1263PP

123. Stadnytskyi V, Bax CE, Bax A, Anfinrud P. The airborne lifetime of small speech droplets and their potential importance in SARS-CoV-2 transmission. *Proc Natl Acad Sci*. 2020;117(22):11875-11877. doi:10.1073/pnas.2006874117

124. World Health Organization. Transmission of SARS-CoV-2: implications for infection prevention precautions. Published July 9, 2020. Accessed January 21, 2021. https://www.who.int/news-room/commentaries/detail/transmission-of-sars-cov-2-implications-for-infection-prevention-precautions

125. Wang W, Xu Y, Gao R, et al. Detection of SARS-CoV-2 in Different Types of Clinical Specimens. *JAMA*. 2020;323(18):1843-1844. doi:10.1001/jama.2020.3786

126. Xiao F, Sun J, Xu Y, et al. Infectious SARS-CoV-2 in Feces of Patient with Severe COVID-19. *Emerg Infect Dis*. 2020;26(8):1920-1922. doi:10.3201/eid2608.200681

127. Zhang Y, Chen C, Zhu S, et al. Isolation of 2019-nCoV from a Stool Specimen of a Laboratory-Confirmed Case of the Coronavirus Disease 2019 (COVID-19). *China CDC Wkly*. 2020;2(8):123-124. doi:10.46234/ccdcw2020.033

128. Elena SF, Sanjuán R. Adaptive Value of High Mutation Rates of RNA Viruses: Separating Causes from Consequences. *J Virol*. 2005;79(18):11555-11558. doi:10.1128/JVI.79.18.11555-11558.2005

129. Peck KM, Lauring AS. Complexities of Viral Mutation Rates. *J Virol*. 2018;92(14). doi:10.1128/JVI.01031-17

130. Ferron F, Subissi L, Morais ATSD, et al. Structural and molecular basis of mismatch correction and ribavirin excision from coronavirus RNA. *Proc Natl Acad Sci*. 2018;115(2):E162-E171. doi:10.1073/pnas.1718806115

131. Baum A, Fulton BO, Wloga E, et al. Antibody cocktail to SARS-CoV-2 spike protein prevents rapid mutational escape seen with individual antibodies. *Science*. 2020;369(6506):1014-1018. doi:10.1126/science.abd0831

132. Zost SJ, Gilchuk P, Case JB, et al. Potently neutralizing and protective human antibodies against SARS-CoV-2. *Nature*. 2020;584(7821):443-449. doi:10.1038/s41586-020-2548-6

133. Yurkovetskiy L, Wang X, Pascal KE, et al. Structural and Functional Analysis of the D614G SARS-CoV-2 Spike Protein Variant. *Cell*. 2020;183(3):739-751.e8. doi:10.1016/j.cell.2020.09.032

134. Zhang L, Jackson CB, Mou H, et al. SARS-CoV-2 spike-protein D614G mutation increases virion spike density and infectivity. *Nat Commun*. 2020;11(1):6013. doi:10.1038/s41467-020-19808-4

135. Laha S, Chakraborty J, Das S, Manna SK, Biswas S, Chatterjee R. Characterizations of SARS-CoV-2 mutational profile, spike protein stability and viral transmission. *Infect Genet Evol*. 2020;85:104445. doi:10.1016/j.meegid.2020.104445

136. Daniloski Z, Jordan TX, Ilmain JK, et al. *The Spike D614G Mutation Increases SARS-CoV-2 Infection of Multiple Human Cell Types*. Genetics; 2020. doi:10.1101/2020.06.14.151357

137. Ozono S, Zhang Y, Ode H, et al. SARS-CoV-2 D614G spike mutation increases entry efficiency with enhanced ACE2-binding affinity. *Nat Commun*. 2021;12(1):848. doi:10.1038/s41467-021-21118-2

138. Hu J, He C-L, Gao Q-Z, et al. D614G mutation of SARS-CoV-2 spike protein enhances viral infectivity. *bioRxiv*. Published online July 6, 2020:2020.06.20.161323. doi:10.1101/2020.06.20.161323

139. Plante JA, Liu Y, Liu J, et al. Spike mutation D614G alters SARS-CoV-2 fitness. *Nature*. Published online October 26, 2020:1-6. doi:10.1038/s41586-020-2895-3

140. Mansbach RA, Chakraborty S, Nguyen K, Montefiori DC, Korber B, Gnanakaran S. The SARS-CoV-2 Spike Variant D614G Favors an Open Conformational State. *bioRxiv*. Published online July 26, 2020:2020.07.26.219741. doi:10.1101/2020.07.26.219741

141. Lorenzo-Redondo R, Nam HH, Roberts SC, et al. A clade of SARS-CoV-2 viruses associated with lower viral loads in patient upper airways. *EBioMedicine*. 2020;62:103112. doi:10.1016/j.ebiom.2020.103112

142. Weissman D, Alameh M-G, de Silva T, et al. D614G Spike Mutation Increases SARS CoV-2 Susceptibility to Neutralization. *Cell Host Microbe*. 2021;29(1):23-31.e4. doi:10.1016/j.chom.2020.11.012